AD-A260 433

||||||||||||||||||||||||||

WL-TR-92-3052

MULTIOBJECTIVE
OPTIMIZATION OF
AEROSPACE STRUCTURES

Ramana V. Grandhi
Geetha Bharatram

Wright State University
Dayton, OH 45435

DTIC
S ELECTE
FEB 0 9 1993
B

JULY 1992

93-02281

|||||||||||||||||||||||||||||||||

FINAL REPORT FOR THE PERIOD JANUARY 1990-DECEMBER 1991

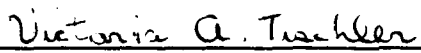APPROVED FOR PUBLIC RELEASE; DISTRIBUTION IS UNLIMITED

FLIGHT DYNAMICS DIRECTORATE

WRIGHT LABORATORY

AIR FORCE SYSTEMS COMMAND

WRIGHT-PATTERSON AIR FORCE BASE, OHIO 45433-6553

NOTICE

When Government drawings, specifications, or other data are used for any purpose other than in connection with a definitely Government-related procurement, the United States Government incurs no responsibility or any obligation whatsoever. The fact that the government may have formulated or in any way supplied the said drawings, specifications, or other data, is not to be regarded by implication, or otherwise in any manner construed, as licensing the holder, or any other person or corporation; or as conveying any rights or permission to manufacture, use, or sell any patented invention that may in any way be related thereto.

This report is releasable to the National Technical Information Service (NTIS). At NTIS, it will be available to the general public, including foreign nations.

This technical report has been reviewed and is approved for publication.

VICTORIA A. TISCHLER
Aerospace Engineer
Design & Analysis Methods Group

NELSON D. WOLF, Technical Manager
Design & Analysis Methods Group
Analysis & Optimization Branch
Structures Division

DAVID K. MILLER, Lt. Col., USAF
Chief, Analysis & Optimization Branch
Structures Division
Flight Dynamics Directorate

If your address has changed, if you wish to be removed from our mailing list, or if the addressee is no longer employed by your organization please notify WL/FIBR , WPAFB, OH 45433- 6553 to help us maintain a current mailing list.

Copies of this report should not be returned unless return is required by security considerations, contractual obligations, or notice on a specific document.

REPORT DOCUMENTATION PAGE

1a. REPORT SECURITY CLASSIFICATION	1b. RESTRICTIVE MARKINGS
UNCLASSIFIED	N/A

2a. SECURITY CLASSIFICATION AUTHORITY	3. DISTRIBUTION/AVAILABILITY OF REPORT
N/A	Approved for Public Release, Distribution is Unlimited
2b. DECLASSIFICATION/DOWNGRADING SCHEDULE	
N/A	

4. PERFORMING ORGANIZATION REPORT NUMBER(S)	5. MONITORING ORGANIZATION REPORT NUMBER(S)
	WL-TR-92-3052

6a. NAME OF PERFORMING ORGANIZATION	6b. OFFICE SYMBOL (If applicable)	7a. NAME OF MONITORING ORGANIZATION
Wright State University	N/A	Flight Dynamics Directorate Wright Laboratory

6c. ADDRESS (City, State, and ZIP Code)	7b. ADDRESS (City, State, and ZIP Code)
Dayton, OH 45435	WL/FIBR Wright-Patterson AFB, OH 45433-6553

8a. NAME OF FUNDING/SPONSORING ORGANIZATION	8b. OFFICE SYMBOL (If applicable)	9. PROCUREMENT INSTRUMENT IDENTIFICATION NUMBER
		F33615-88-C-3204

8c. ADDRESS (City, State, and ZIP Code)	10. SOURCE OF FUNDING NUMBERS			
	PROGRAM ELEMENT NO.	PROJECT NO.	TASK NO.	WORK UNIT ACCESSION NO
	61102F	2302	N5	08

11. TITLE (Include Security Classification)

Multiobjective Optimization of Aerospace Structures

12. PERSONAL AUTHOR(S)
Ramana V. Grandhi and Geetha Bharatram

13a. TYPE OF REPORT	13b. TIME COVERED	14. DATE OF REPORT (Year, Month, Day)	15. PAGE COUNT
Final	FROM 1 JAN 90 TO 31 DEC 91	July 1992	120

16. SUPPLEMENTARY NOTATION

17	COSATI CODES		18. SUBJECT TERMS (Continue on reverse if necessary and identify by block number)
FIELD	GROUP	SUB-GROUP	Structural Optimization Reliability Design
01	04		Compound Scaling
			Finite Element Analysis

19. ABSTRACT (Continue on reverse if necessary and identify by block number)

This report presents the multiobjective optimization methodology suitable to the preliminary design of large scale aircraft structures. The algorithm is based on generalized compound scaling techniques to reach the intersection of multiple functions. Multiobjective functions are treated similar to the behavior constraints by generating pseudo targets on objectives. This algorithm is very efficient due to the fact that it does not solve many single objective optimization problems in reaching the Pareto set. The Pareto set gives several optimum solutions, and the designer has to use additional decision criteria in selecting the best design. In this work a reliability index based concept is used as the decision criterion. System reliability of the Pareto designs is calculated due to the random nature of material properties, fabrication tolerances, and service loads, where the random parameters influencing the design appear through their mean and covariance values.

20. DISTRIBUTION/AVAILABILITY OF ABSTRACT	21. ABSTRACT SECURITY CLASSIFICATION
☒ UNCLASSIFIED/UNLIMITED ☐ SAME AS RPT. ☐ DTIC USERS	UNCLASSIFIED
22a. NAME OF RESPONSIBLE INDIVIDUAL	22b. TELEPHONE (Include Area Code)	22c. OFFICE SYMBOL
Victoria A. Tischler	(513)255-6992	WL/FIBR

DD FORM 1473, 84 MAR   83 APR edition may be used until exhausted.   SECURITY CLASSIFICATION OF THIS PAGE
All other editions are obsolete.

FOREWORD

DTIC QUALITY INSPECTED 3

Accession For

NTIS GRA&I	☑
DTIC TAB	☐
Unannounced	☐
Justification	

By

Distribution/

Availability Codes

| Dist | Avail and/or Special |
| A-1 | |

CONTENTS

FIGURES

TABLES

x

SECTION 1

INTRODUCTION

Multiobjective optimization has recently been acknowledged as an advanced design technique in structural optimization. Most of the real world problems are multidisciplinary and complex, there are always more than one important objective function in the problem. In order to accomodate many conflicting design goals, one needs to formulate the optimization problem with multiple objectives. Formulation of a structural optimization problem consists of constructing a mathematical model that describes the behavior of a physical system encompassing the problem area. The main task is the determination of the choice of the design variables, objectives and the constraints. Sometimes only one dominating criterion may be a sufficient objective for minimization. This is true especially if the other requirements can be presented by equality and inequality constraints. But generally the choice of the constraint limits may be a difficult task in a practical design problem. These allowable values can be rather *fuzzy* even for common quantities such as displacements, stresses, and natural frequencies. If the limit cannot be determined, it seems reasonable to treat that quantity as an objective.

1

In addition, usually several competing and noncommensurable objectives appear in a real-life application, and thus the designer is faced with a decision making problem where the task is to find the best compromise solution between the conflicting requirements. Many methods have been developed to help the engineer make the right decision in conflicting situations.

In the majority of the publications dealing with structural optimization the objective, which should be minimized, has been the structural weight. In many civil and mechanical engineering applications, the manufacturing cost may be conflicting with the weight which does not reflect the total cost of the structure. Accordingly, from the purely economic viewpoint the weight represents only the material cost and therefore additional criteria are needed. When formulating the mathematical optimization problem, the designer must consider which quantities are suitable for measuring the economy and the performance of the structure. Any quantity which has a tendency to improve or deteriorate is actually an objective function in nature. Those quantities which should only satisfy some imposed requirements are not objectives and can be treated as constraints. In a strict sense, almost all design quantities have a criterion nature rather than a constraint nature, because in the designer's mind they usually have better or worse values. As an example of a strict constraint, the structural analysis equations (displacement, stresses etc.) can be mentioned. They represent equality constraints, whereas regulations, space limitations, available materials and manufacturing techniques impose inequality constraints. Thus the designer is usually faced with several conflicting and non-commensurable objectives in formulating

the optimization problem. In order to reduce the computational and decision-making effort it is desirable to decrease the number of the objectives as far as possible by moving them into constraints.

A general multiobjective optimization problem is to find the vector of design variables $X = (x_1, x_2, ..., x_N)^T$ which minimizes a vector objective function $F(X) = (F_1(X), F_2(X), ..., F_q(X))^T$ over the feasible design space X. It is the determination of a set of non-dominated solutions (or Pareto optimum solutions, noninferior solutions or efficient solutions) that achieves a compromise among several different, usually conflicting, objective functions. The non-dominated solutions form a set of solutions in which no decrease can be obtained in any of the objectives without causing a simultaneous increase in at least one of the objectives. This definition can be understood graphically. An arbitrary collection of feasible alternatives for a two-objective maximization problem is shown in Figure 1.1. The area inside of the shape and its boundaries are feasible. The axes of this graph are the objectives F_1 and F_2. It can be clearly seen from the graph that the noninferior solutions are found in the portion of the boundary between points A and B. Thus, here arises the decision making problem from which a partial or complete ordering of the set of non-dominated objectives is accomplished by considering the preferences of the decision maker. Most of the multiobjective optimization techniques are based on how to elicit the preferences and determine the best compromise solution.

3

1.1 Literature Review

A variety of techniques and applications of multiobjective optimization have been developed in the past few years. The earliest work reporting the consideration of multiple objectives in mathematical programming appears to be that of Kuhn and Tucker (1951). Progress in the field of multicriteria optimization was summarized by Hwang and Masud (1979) and later by Stadler (1984,1987). Stadler inferred from his survey that if one has decided that an optimal design is to be based on the consideration of several criteria, then the multicriteria theory (Pareto theory) provides the necessary framework. In addition, if the minimization or maximization is the objective for each criterion, then an optimal solution should be a member of the corresponding Pareto set, for only then does any further improvement in one criterion require a clear trade-off with at least one other criterion. He also observed that in mechanics the most widely used technique was goal programming. Bartel and Marks (1974) developed a method for analyzing optimum design problems with multiple, competing objective functions. The technique provides a method for displaying the trade-off between two competing design objectives over the whole range of the design space. The resulting trade-off curve gives the designer the best possible choices for compromise designs. The usefulness of this method was demonstrated by applying it to the optimum design of hydrodynamic journal bearings. The competing objectives were to minimize the oil film temperature rise and to minimize the oil flow rate for the constant loading case. Duckstein (1984) listed about 13 possible sample multiobjective techniques to show that a fairly broad choice of approach is to

4

structural design is possible. Radford, .et.al. (1985) in their study have explored the role of Pareto optimization in CAD. They used the weighting, NonInferior Set Estimation Method (NISE), and the constraint method for generating the Pareto optimal, and suggested some approaches using the emerging field of knowledge based engineering to formalize the control and derivation of meaning from the Pareto sets.

Rao (1984,1987,1988) has done a considerable amount of study on multiobjective optimization. In most of his research work goal programming and game theory techniques were used. Rao (1984) studied the application of multiobjective optimization to structural design problems involving uncertain parameters and random processes. The design of a cantilever beam with a tip mass subjected to a stochastic base excitation was considered for illustration. The objectives in the problem were to minimize structural mass, maximize the fundamental natural frequency and minimize fatigue damage time. He obtained numerical results using a number of methods and concluded that the game theory approach was superior in finding a better optimum solution with proper balance of the various objective functions, even though the computation time was high compared to the other methods discussed in his work. It was also observed that the optimum solutions given by the various multicriteria optimization methods can be different. Rao (1987) proposed a computational procedure for solving a general multiobjective optimization problem using cooperative game theory. He presented graphical interpretations of the non-cooperative and cooperative game theory approaches for a two-criteria problem. Later he and his co-workers (1988) formulated the

design of actively controlled structures subject to restrictions on the damping parameters of the closed-loop system as a multiobjective optimization problem and solved it using goal programming techniques. The purpose of the control was to effectively suppress structural vibrations due to initial excitation. The structural weight and the controlled system energy were considered as the objective functions for minimization. Rao, *et.al.* (1988) formulated a combined structural/control optimization problem and solved it as a multiobjective optimization problem. The authors used the game theory approach for generating the Pareto optimal. The computational procedure was demonstrated through the design of two actively controlled truss structures. The two objective functions used for the optimization were to minimize the weight of the structure as well as the quadratic performance index. Rao (1988) considered the design of vibration isolation systems using multicriteria optimization techniques. The two performance indices taken as the objective functions were the integrated values of the force transmitted to the main mass and the relative displacement between the main mass and the base. He demonstrated the applicability of global criterion, bounded objective, utility function, and game theory methods in the design of a multicriterion vibration isolation system.

The multicriterion optimization of elastic stress limited isostatic trusses was considered, and a numerical method (weighting method, constraint method, etc.) for determining the Pareto optimal set of the problem was developed by Koski (1982,1983). He discussed the basic principles of multicriterion optimization

and presented Pareto optima using the weighting as well as the minimax approaches (1981,1984). Hyperstatic trusses and plane frames were designed where the weight and some chosen nodal displacements of the structure were taken as design criteria. He also suggested that generating the whole Pareto set was not economical, therefore to reduce the number of Pareto optima generated, one could develop interactive algorithms where only a few Pareto optimal solutions were generated. Later in (1984) he developed an interactive design method for truss optimization. Koski (1987) proposed the norm methods based on the scalarization of the original multicriterion problem by using the l_p-norm method also called the global criterion method. In addition, an alternative approach which, instead of scalarization, reduces the dimension of the multicriterion problem was proposed. He called this method the partial weighting method. Throughout the article several illustrative truss examples were presented. In addition to interactive multiobjective optimization methods Diaz (1987) proposed sensitivity analysis as a useful tool for information regarding trade-offs in the objectives. Hajela and Shih (1990) proposed a minimum variant of the global criterion approach to obtain solutions to multiobjective optimum design problems involving a mix of continuous, discrete, and integer design variables. The method combined a discrete variable variant of the global criterion approach with a branch-and-bound strategy.

El-Sayed, *et.al.* (1989) demonstrated the formulation of the nonlinear goal optimization problem and demonstrated the use of the method, as a design tool.

Sandgren (1989) introduced a means by which uncertainty in the optimal design of structures could be considered. A goal programming formulation was generated for a three-bar truss problem wherein uncertainty in both the load magnitude and direction was considered. He demonstrated that nonlinear goal programming could be a valuable tool for designing under uncertainty conditions. Also this approach significantly reduces the complexity of the solution process. Dhingra, *et.al.* (1989) presented fuzzy optimization techniques and summarized their work as an useful tool during the initial stages of the conceptual design of engineering systems where the design goals and the constraints have not been clearly defined. Saravanos and Chamis (1990) developed a methodology for light weight low cost composite structures of improved dynamic performance. Preliminary applications on a cantilever composite beam illustrated that only the proposed multiobjective optimization improved all objectives simultaneously as opposed to single objective functions. Tseng and Lu (1990) proposed a minimax multiobjective optimization model for structural optimization. They used the three typical multiobjective optimization techniques, goal programming, compromise programming and the surrogate worth trade-off method, to solve truss problems. The main purpose of their work was to apply the multiobjective optimization techniques to the selection of system parameters and to solve large scale structural design optimization problems.

1.2 Types of Multiobjective Techniques

Pareto optimality serves as the basic multicriteria optimization concept in

virtually all of the previous literature. Pareto presented a qualitative definition of the optimality concept for economic problems with several conflicting objectives. The Pareto optimal is stated in simple words as, "A vector X^* is Pareto optimal if there exists no feasible vector X which would decrease some objective function without causing a simultaneous increase in at least one objective function". These solutions are also called noninferior solutions or non-dominated solutions.

Nearly all of the definitions of optimality in use for multiobjective optimization involve some sort of scalarization of the vector optimization problem. That is, the replacement of the vector problem by some equivalent scalar minimization problem. Also the Pareto set is generally infinite. An additional use of scalarization is the selection of a unique member of the Pareto set as the optimum for the vector optimization problem. Usually, a problem is scalarized either by defining an additional super criterion function or by considering the criteria sequentially.

The basic three techniques used for generating noninferior solutions are: the weighting method, the NonInferior Set Estimation method (NISE) and the constraint method. Balachandran and Gero (1987) have discussed the relative merits and demerits of these three methods. These methods also come under the category of nonpreference techniques. Although, one should note that some nonpreference techniques use preference techniques concepts repeated over a number of different parametric values to generate the entire Pareto set. Figure 1.2.1 shows the procedure used in multiobjective optimization in structural optimization. In the following sections these methods are briefly discussed with goal programming, game theory, global criterion etc.

Weighting Method

This technique is based on the preference techniques of prior assessment of the weights. It transforms the multicriteria function to a single criterion function through a parameterization of the relative weighting of the criteria. The problem can be stated as:

Minimize

$$F(X) = \sum_{k=1}^{q} W_k F_k(X) \tag{1}$$

subject to

$$g_i(X) \geq 0 \qquad i = 1, 2, \dots m \tag{1.a}$$

It is usually assumed that

$$0 \leq W_k \leq 1, \qquad \sum_{k=1}^{q} W_k = 1 \tag{1.b}$$

where X are the design variables, and W are the weights for each of the q objective functions. With the variation of the weights the entire Pareto set can be generated. Since the results of solving an optimization problem can vary significantly as the weighting coefficients change, and since very little is usually known about how to choose these coefficients, a necessary approach is to solve the same problem for many different values of weighting factors. However, since the shape and distribution characteristics of the Pareto set are unknowns, it is impossible to determine beforehand the nature of the variations required in the weights so as to produce a new solution at each pass. The second important disadvantage of the method is that it will not identify Pareto solutions in a nonconvex part of

10

the set. Still confronted with these Pareto solutions, the designer must choose among them by some other means.

NonInferior Set Estimation (NISE) Method

The NISE method (Cohon, 1978) is an extension of the weighting method with a mechanism for quickly converging onto the Pareto set. In addition, the accuracy of the approximation can be controlled in the NISE method through a predetermined error criterion, which is compared to the maximum possible error at every iteration of the method. The NISE method operates by finding a number of noninferior extreme points and evaluating the properties of the line segments between them. For example if two noninferior extreme points have been found, then the segment between them is feasible and it may or may not be inferior. If the line segment is noninferior, then moving in a direction out from the line segment is infeasible. If the line segment is inferior, then there are noninferior points in the outward direction. Noninferior points are found in the NISE method through the use of the weighting method.

Constraint Method

The constraint method is discussed in more detail, since Pareto solutions are generated using this technique for a few examples in the report for comparisons with the proposed generalized compound scaling technique. The constraint method is a technique which transforms a multicriteria objective function into a single criterion by retaining one selected objective as the primary criterion to be

optimized and treating the remaining criteria as constraints. The multicriteria problem is thus stated as:

Minimize

$$F_1(X) \tag{2}$$

subject to the constraints

$$F_i(X) \geq b_i \quad i = 2, 3, ..., q \tag{2.a}$$

$$g_i(X) \geq 0 \quad i = 1, 2, ...m \tag{2.b}$$

and the side bounds on the design variables as

$$x_i \geq x_i^{(l)} \quad i = 1, 2, ..., n \tag{2.c}$$

where b_i are parametrically varied target levels of the $q - 1$ objective functions. Each vector, or constraint set, B of the various b_i will produce one Pareto solution. As in the weighting method, many different combinations of values for each b_i must be examined in turn to generate the entire Pareto set. The constraint method provides direct control of the generation of members of the Pareto set and generally provides an efficient method for defining the shape of the Pareto set.

Multiobjective optimization that incorporates preferences is described below. The commonly used methods under this are: goal programming, game theory, global criterion, and the surrogate worth trade-off method.

Goal Programming

In goal programming the decision maker is required to specify goals for each objective that he wishes to attain. Goals are the quantitative values, considered as additional constraints in which new variables are added to represent deviations from the predetermined targets. The objective function specifies the deviations from these goals and priorities for the achievement of each goal, in quantitative terms. Thus, the goal programming formulation of the multiobjective optimization problem leads to:

Minimize

$$[\sum_{j=1}^{q} (d_j^+ + d_j^-)^p]^{\frac{1}{p}}, \qquad p \geq 1 \tag{3}$$

subject to

$$g_j(X) \geq 0 \qquad j = 1, 2, ..., m \tag{3.a}$$

$$F_j(X) - d_j^+ + d_j^- = b_j, \qquad j = 1, 2, ..., q \tag{3.b}$$

$$d_j^+ \geq 0, \qquad j = 1, 2, ..., q \tag{3.c}$$

$$d_j^- \geq 0, \qquad j = 1, 2, ..., q \tag{3.d}$$

where b_j is the goal set by the designer for the jth objective, and d_j^+ and d_j^- are, respectively, the under- and over- achievement of the jth goal. The value of p is based upon the utility function chosen by the designer. Generally, $p = 2$ which is an Euclidean metric value. The disadvantages of this method are the selection of "correct" or "valid" levels of d^+ and d^-, i.e, which requires knowledge of the individual minima of the objective function which is not easy to achieve with nonconvex problems.

Game Theory

In game theory, the multiobjective optimization problem is viewed as a game problem involving several players, each corresponding to one of the objectives. The system is considered to be under the control of these intelligent adversaries, each seeking to optimize his own gain at the expense of his opponents, using all the available information. In this approach, starting with X_0 as a starting point, q single criterion optimization problems are solved to obtain optimum solutions $X_i^*, i = 1, 2, ..., q$. With the help of X_i^* the elements of the matrix $[P]$ are evaluated as

$$[P] = \begin{bmatrix} F_1(X_1^*) & F_2(X_1^*) & ... & F_q(X_1^*) \\ F_1(X_2^*) & F_2(X_2^*) & ... & F_q(X_3^*) \\ . & & & \\ . & & & \\ . & & & \\ F_1(X_q^*) & F_2(X_q^*) & ... & F_q(X_q^*) \end{bmatrix} \qquad (4.a)$$

From this matrix the largest element of the i th column, F_{iu} is selected from each column (worst value). Then a supercriterion or bargaining model S is constructed as

$$S = \Pi_{i=1}^q [F_{iu} - F_i(X_c^*)] \qquad (4.b)$$

where X_c^* represents the solution (Pareto optimal solution) of the following problem.

Minimize

$$F_c(c, X) = \sum_{i=1}^{q-1} c_i F_i(X) + (1 - \sum_{i=1}^{q-1} F_i(X)) \qquad (4.c)$$

14

subject to

$$g_i \geq 0, \qquad i = 1, 2, ..., m \tag{4.d}$$

$$c_i \geq 0, \qquad i = 1, 2, ..., q - 1 \tag{4.e}$$

$$\sum_{i=1}^{q-1} c_i \leq 1 \tag{4.f}$$

The supercriterion S defined in Eq (4.b) is maximized, the optimal convex combination of the objective functions is found, that is, c^* and the corresponding optimum solution of the problem $X^* = X_c^*$ is determined.

Surrogate Worth Trade-off Method

The surrogate worth trade-off (SWT) method is an interactive method, which can be applied when the design variables are continuous and the objective functions and constraints are twice differentiable. It assumes that the preference of the decision maker is monotonic and can be exhibited as an implicit multiattribute utility function as the decision maker systematically compares two objectives at a time. The SWT method consists of three main steps. First, generating a representative subset of non-dominated solutions called promising solutions and obtaining the relevant trade-off information for each generated solution. Second, interacting with the decision maker to elect the preference structure and finally, selecting the best-compromise solution from the information obtained. Using the constraint method the promising solutions and also the associated trade-off information are generated. By using the concept duality theory, the Lagrange

15

multipliers as well as the Kuhn-Tucker conditions, the trade-off functions T_{ij} are defined as

$$T_{ij} = \frac{\partial f_i(X)}{\partial f_j(X)} \qquad (5.a)$$

or

$$T_{ij} = -\Lambda_{ij} \qquad (5.b)$$

Λ_{ij} is the generalized Lagrange multiplier associated with the ith constraint. The trade-off Λ_{ij} represents the marginal rate of substitution between the ith and jth objectives. Once the trade-offs have been identified, the decision maker is supplied with the trade-off information to express his ordinal preference.

Global Criterion Method (min-max formulation)

In this formulation the optimum solution X^* is found by minimizing a pre-selected global criterion $\tilde{F}(X)$ such as, the sum of the squares of the relative deviations of the individual objective functions, from the feasible ideal solutions. Thus X^* is found by minimizing

$$\tilde{F}(X) = \sum_{i=1}^{q} \left(\frac{F_i(X_i^*) - F_i(X)}{F_i(X_i^*)} \right)^p \qquad (6.a)$$

subject to

$$g_i(X) \geq 0, \qquad i = 1, 2, ..., m \qquad (6.b)$$

where p is generally taken as 2, $X_i^*, i = 1, 2, ..., q$ is the feasible ideal solution of the i th objective, and it is obtained by minimizing individual criterion.

16

1.3 Scope of the Work

As shown from the description of the methods, there are various drawbacks in using these approaches for solving large scale multidisciplinary optimization problems with finite element based analyses. For example, many single objective optimization problems have to be solved for generating the Pareto set in the constraint method. Different weights have to be associated with the objectives to obtain the Pareto set in the weighting method. In goal programming, game theory, and global criterion methods individual minima's of the single objective function are required which are difficult to obtain for a nonconvex problem. Hence, it can be seen that multiobjective optimization can become computer intensive while generating the Pareto optimal set.

This work proposes an algorithm ideally suited for multicriteria optimization. This algorithm is based on the generalized compound scaling (Venkayya, 1989-1991) method where the objectives are treated as similar to constraints. A partial Pareto optimal set is generated by the algorithm. The computational cost involved in this method is much smaller than the other methods discussed. This is because in one optimization problem, possible Pareto optimums are generated. The knowledge of individual minima's is not necessary for this algorithm, thus opening a wide range of problems that can be solved using this technique. The algorithm works well, because the optimal solutions lie on the active constraint boundary for structural optimization problems whether the optimization is single objective or multiobjective. In this work different objective functions (linear and nonlinear) were used to show the robustness of the algorithm.

17

This report is divided into many sections. The main sections being the finite element formulation for the plate element, the sensitivity calculations for the objective functions and the constraints, the multiobjective optimization algorithm with mathematical details, and numerical results with relevant discussions.
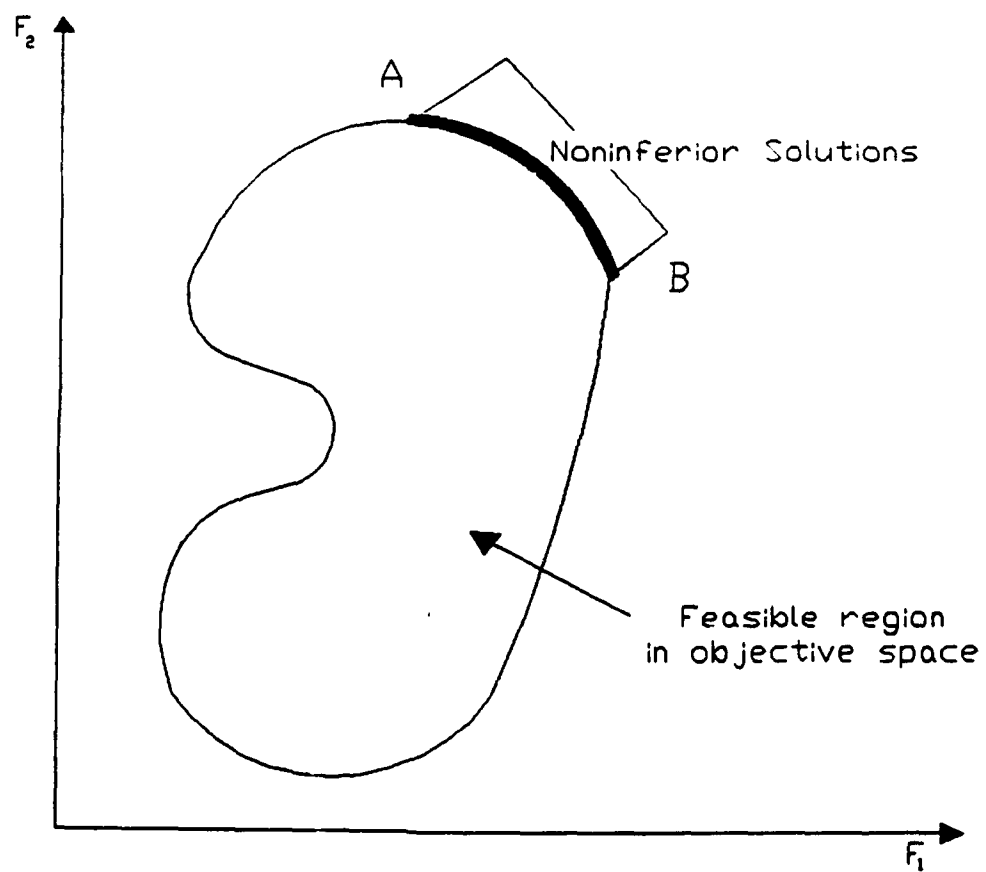
Fig. 1.1 Graphical interpretation of Pareto Optimal

19

```
┌─────────────────────────────────────────────────────┐
│              Problem  Formulation                     │
│                                                       │
│    Min [ f₁(x)    f₂(x) . . .    fₘ (x) ]ᵀ            │
└─────────────────────────────────────────────────────┘
                        │
                        ▼
┌─────────────────────────────────────────────────────────────────┐
│              Generation of  Pareto  optima                        │
├──────────┬───────────┬─────────────┬────────┬───────────┬────────┤
│Constraint│ Global    │ Goal        │ Game   │ Surrogate │Weighting│
│method    │ Criterion │ Programming │ Theory │ worth     │method   │
│          │ method    │             │        │ trade-Off │         │
└──────────┴───────────┴─────────────┴────────┴───────────┴────────┘
                        │
                        ▼
┌─────────────────────────────────────────────────────┐
│              Decision  making                         │
├──────────────────┬──────────────────┬────────────────┤
│ Interactive      │ Choice by        │ A  priori      │
│ methods          │ comparisons      │ fixed          │
│                  │                  │ parameters     │
└──────────────────┴──────────────────┴────────────────┘
```

$$\text{Min} \; [\, f_1(x) \quad f_2(x) \; \ldots \; f_m(x) \,]^T$$
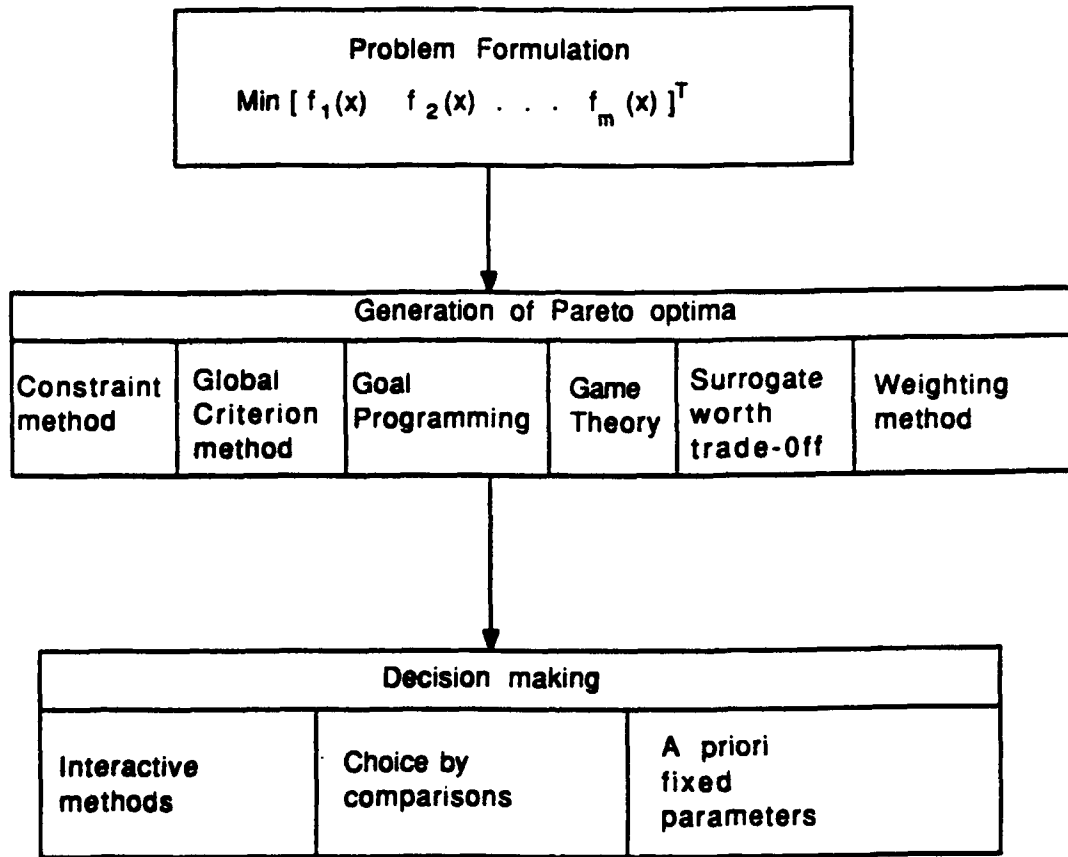
Fig. 1.2.1   Classification of multicriterion structural design process

SECTION 2

FINITE ELEMENT FORMULATION

This section discusses the finite element approximations used in the present study. The choice of elements is dictated by the need to perform accurate solutions for both thin and thick plates. The finite element used for the plate bending elements is a four noded , bilinear displacement element based on the Mindlin plate theory (Mindlin 1951). A reduced integration scheme is used to evaluate the element matrices. This results in a rank-deficient element , and must be stabilized to achieve reliable behavior.

The theory of single-point quadrature was introduced by Hughes, *et.al.* (1978) and designated as U1. This element was attractive because of its simplicity, computational efficiency, and high accuracy. However the U1 element is rank deficient as this element cannot capture the bilinear contributions to the displacement fields due to the single-point integration. Therefore, this element leads to some spurious oscillatory displacements with very little strain energy associated with it. These spurious singular modes in structural mechanics are called hourglass modes or zero energy modes. Because of this a structure that appears adequately constrained may yet have an instability that makes the [K] singular.

21

The control method used to eliminate instability is by providing restraint without stiffening the element's response to modes of behavior that are working well. The method adds "hourglass stiffness" to an element integrated by one - point quadrature . For a four noded bilinear rectangular plate element eight independent displacement modes can be identified as shown in the Figure 2.1. The first three are rigid body modes for which the strain energy is zero. The next three modes are constant strain energy modes. Modes 7 and 8 are bending modes. An order of one point quadrature does not sense these two modes, as the Gauss point is at the center of the element and hence $\epsilon_x = \epsilon_y = \gamma_{xy} = 0$ at the center. Accordingly, the strain energy for these two modes is zero or almost equal to zero, hence the element displays two mechanisms (Cook, *et.al.*, 1989). Therefore to provide mode 7 and mode 8 with stiffness they lack under single-point quadrature, a "stabilization matrix " is formed for each mode. These matrices contain constants which can be chosen such that a rectangular element displays the exact strain energy in states of pure bending (Belytschko and Tsay, 1983). These correction stiffness matrices are added to the element stiffness matrix. For stress computations (especially shear stresses) the one point quadrature technique is the most accurate.

The bilinear Mindlin plate (BMP) elements used in PROTEC (Brockman, *et.al.*, 1989) are based upon uniform reduced integration with rank corrections. The BMP bending element uses single point quadrature. The rank correction scheme uses five generalized hourglass strains to complement the proper null space of the reduced integrated Mindlin plate gradient operator.

2.1 Plate Element

In the Mindlin plate theory transverse shear deformation are also taken into consideration. Therefore any point not on the midsurface is not governed by slopes $w_{,x}$ and $w_{,y}$ but is governed by rotations θ_x and θ_y of lines that were normal to the midsurface of the undeformed plate.

$$
\begin{aligned}
u &= -z\theta_x & \epsilon_x &= -z\theta_{x,x} & \gamma_{xy} &= -z(\theta_{x,y} + \theta_{y,x}) \\
v &= -z\theta_y & \epsilon_y &= -z\theta_{y,y} & \gamma_{yz} &= w_{,y} - \theta_y \\
& & & & \gamma_{xz} &= w_{,x} - \theta_x
\end{aligned}
$$

$$(7)$$

The state of deformation is described by generalized strains,

$$\epsilon^t = [\epsilon_x, \epsilon_y, \gamma_{xy}, k_x, k_y, k_{xy}, \gamma_{xz}, \gamma_{yz}] \tag{8}$$

and the stress state by generalized forces,

$$\sigma^t = [N_x, N_y, N_{xy}, M_x, M_y, M_{xy}, Q_{xz}, Q_{yz}] \tag{9}$$

In the stress-strain relationships for the in-surface strains and curvatures, plane stress assumptions are used. For the bilinear plate element the shape functions are,

$$N_i = \frac{1}{4}(s + \xi\xi + \eta\eta + h\eta\xi) \tag{10}$$

Expanding the shape function one can write

$$N_1 = \frac{1}{4}(1 - \eta)(1 - \xi) \tag{10.a}$$

23

$$N_2 = \frac{1}{4}(1 + \eta)(1 - \xi) \qquad (10.b)$$

$$N_3 = \frac{1}{4}(1 + \eta)(1 + \xi) \qquad (10.c)$$

$$N_4 = \frac{1}{4}(1 - \eta)(1 + \xi) \qquad (10.d)$$

In Eq (10) rigid body modes are denoted by

$$s^t = [1, 1, 1, 1] \qquad (11.a)$$

the nodal coordinates in the reference planes are,

$$\xi^t = [-1, 1, 1, -1] \qquad (11.b)$$

$$\eta^t = [-1, -1, 1, 1] \qquad (11.c)$$

and the hour glass modes are (see Figure 1.2 mode 7 and 8)

$$h^t = [1, -1, 1, -1] \qquad (11.d)$$

For the plate element the membrane strains from Eq (7) are given by

$$\epsilon_m = \begin{pmatrix} \epsilon_x \\ \epsilon_y \\ \gamma_{xy} \end{pmatrix} = \begin{pmatrix} \frac{\partial u}{\partial x} \\ \frac{\partial v}{\partial y} \\ \frac{\partial u}{\partial y} + \frac{\partial v}{\partial x} \end{pmatrix} \qquad (12)$$

and the corresponding elastic matrix D_m is

$$[D_m] = \frac{Et}{(1 - \nu^2)} \begin{bmatrix} 1 & \nu & 0 \\ \nu & 1 & 0 \\ 0 & 0 & \frac{1-\nu}{2} \end{bmatrix} \qquad (13)$$

The bending and shear strains are based on the Hellinger-Reissnar variational principle.

24

Bending strains

$$k = \begin{pmatrix} k_x \\ k_y \\ k_{xy} \end{pmatrix} \qquad (14.a)$$

$$= \begin{pmatrix} \frac{\partial \theta_x}{\partial x} \\ \frac{\partial \theta_y}{\partial y} \\ \frac{\partial \theta_x}{\partial y} + \frac{\partial \theta_y}{\partial x} \end{pmatrix} \qquad (14.b)$$

Shear strains

$$\epsilon_s = \begin{pmatrix} \gamma_{xz} \\ \gamma_{yz} \end{pmatrix} = \begin{pmatrix} \frac{-\partial w}{\partial x} + \theta_x \\ \frac{-\partial w}{\partial y} + \theta_y \end{pmatrix} \qquad (15)$$

The bending elastic matrix D_b is

$$[D_b] = \frac{t^2}{12}[D_m] \qquad (16)$$

The shear elastic matrix D_s is

$$[D_s] = \left(\frac{5}{6}\right)\frac{Et}{2(1+\nu)}\begin{bmatrix} 1 & 0 \\ 0 & 1 \end{bmatrix} \qquad (17)$$

where $\frac{5}{6}$ is the shear correction for isotropic plates(Whitney, 1973). The linear elastic relations take the form

$$(n) = \begin{pmatrix} N_x \\ N_y \\ N_{xy} \end{pmatrix} = D_m \epsilon_m \qquad (18.a)$$

$$(m) = \begin{pmatrix} M_x \\ M_y \\ M_{xy} \end{pmatrix} = D_b k \qquad (18.b)$$

$$(q) = \begin{pmatrix} Q_x \\ Q_y \end{pmatrix} = D_s \epsilon_s \qquad (18.c)$$

25

The strain-displacement matrix evaluated at the center can be written as (Brockman, *et.al.*, 1989)

$$\mathbf{B} = \begin{pmatrix} b_1{}^T & 0 & 0 & \zeta & 0 & 0 \\ 0 & b_2{}^T & 0 & 0 & 0 & 0 \\ b_2{}^T & b_1{}^T & 0 & 0 & 0 & 0 \\ 0 & 0 & 0 & 0 & b_1{}^T & 0 \\ 0 & 0 & 0 & -b_2{}^T & 0 & 0 \\ 0 & 0 & 0 & -b_1{}^T & b_2{}^T & 0 \\ 0 & 0 & b_1{}^T & 0 & \frac{1}{4}s^T & 0 \\ 0 & 0 & b_2{}^T & \frac{-1}{4}s^T & 0 & \zeta \end{pmatrix} \tag{19}$$

In Eq (19)

$$b_1{}^T = \frac{1}{2}[(y_2 - y_1),(y_3 - y_1),(y_4 - y_2),(y_1 - y_3)] \tag{20.a}$$

$$b_2{}^T = \frac{1}{2}[(x_4 - x_2),(x_1 - x_3),(x_2 - x_4),(x_3 - x_1)] \tag{20.b}$$

$\xi = \eta = 0$ (at the center of the element).

$$b_1 = [\frac{\partial N}{\partial x}] \tag{21.a}$$

$$b_2 = [\frac{\partial N}{\partial y}] \tag{21.b}$$

The element displacement vector

$$U^t = [u,v,w,\theta_x,\theta_y,\theta_z] \tag{22}$$

The element stiffness matrix is

$$[K_e] = \int [B]^T[D][B]dv \tag{23}$$

$$\mathbf{K} = \mathbf{B^T DBA}|\mathbf{J}| \tag{24}$$

26

D is the elastic matrix of the element which consists of D_m, D_b, and D_s, A is the area of the element and J is the jacobian. The K_e matrix is a (24 x 24) matrix.

The static equilibrium for the structure is

$$[\mathbf{K}]\mathbf{U} = \mathbf{P} \tag{25}$$

where K is the global stiffness matrix. From equation (25) the nodal displacements are determined as

$$\mathbf{U} = \mathbf{K}^{-1}\mathbf{P} \tag{26}$$

The Moment-Curvature relation from Eqs (18.a-c) yields the stress resultants which are

$$\begin{Bmatrix} N_x \\ N_y \\ N_{xy} \\ M_x \\ M_y \\ M_{xy} \\ Q_x \\ Q_y \end{Bmatrix} = DBU_e \tag{27}$$

where U_e are the nodal displacements for the element.

2.2 Stabilization of the Stiffness Matrix

The plate element consists of twenty four degrees of freedom. Ignoring the θ_z degree of freedom the plate element consists of six rigid body modes , eight uniform strain modes captured by the one point integration and six spurious zero energy modes. The six zero energy modes have to be stabilized.

The six rigid body modes are translations and rotations along the x, y,and z axes. The hour glass modes can be represented by eqn(11.d). The six spurious modes consist of five hourglass deformation patterns

$$u = h, v = h, w = h, \theta_z = h, \theta_y = h \tag{28}$$

The sixth spurious mode cannot exist when a mesh of two or more exist.

To control the kinematic modes, generalized strains are defined which get activated during the zero energy modes and vanish for rigid body modes. Belytschko and Tsay (1981,1983) defined generalized hourglass strains associated with each component of displacement and rotation. These are defined as follows.

$$q_1 = \gamma^T u, \; q_2 = \gamma^T v, \; q_3 = \gamma^T w, \; q_4 = \gamma^T \theta_z, \; q_5 = \gamma^T \theta_y.$$

where

$$\gamma = h - \frac{1}{A}[h^T x b_1 + h^T y b_2] \tag{29}$$

Equation (29) is valid because of the orthogonality conditions. The generalized hourglass stiffness associated with the modes described in Eq (28) are

$$\begin{pmatrix} E_1 \\ E_2 \\ E_3 \\ E_4 \\ E_5 \end{pmatrix} = \frac{0.1 E t A}{1 + \frac{1}{A}} \begin{pmatrix} 1 \\ 1 \\ \frac{t^2}{12} \\ \frac{t^2}{12} \\ \frac{t^2}{12} \end{pmatrix} \tag{30}$$

These stiffnesses are added to the original stiffness matrix.

28

2.3 Mass Matrix Formulation

In static problems the stabilization scheme mentioned (Brockman, *et.al.*, 1987) works perfectly, giving good element behaviour. In dynamics, however, low-energy deformation patterns consisting mainly of hourglassing motions represent likely modes of low-frequency oscillations. These low frequency oscillations contaminate the vibration spectrum which is of the most interest.

This can be shown by the following method. Given a vibration mode shape $d = \Phi$, the generalized stiffness and mass associated with the mode are the projections:

$$k = \Phi^t K \Phi \qquad m = \Phi^t M \Phi \qquad (31)$$

and the corresponding frequency of vibration is

$$\omega = \sqrt{\frac{k}{m}} \qquad (32)$$

Since the hourglass modes are orthogonal to the constant strain modes and rigid body modes, the stiffness associated with these modes depends solely on the hourglass stiffness which is deliberately made small to avoid locking problems. But at the same time the kinetic energy associated with these unstable modes is similar in magnitude to that associated with the rigid body and uniform state motions. This is because the orthogonality conditions are no longer existing while calculating the kinetic energy of the system. Consequently artificial vibrations modes appear in the element spectrum , intermixed with the lower fundamental frequency modes which are commonly of interest.

29

Hence during the mass matrix formulation the mass matrix has to be corrected by reducing or eliminating the kinetic energy associated with unstable modes of the element, while leaving the energy associated with rigid body motions and uniform strain states unchanged (Brockman, et.al., (1987)).

For the mass properties of the bilinear element

$$(R_1, R_2, R_3) = \int_{\frac{-t}{2}}^{\frac{t}{2}} \rho(1, z, z^2) dz \tag{33}$$

and

$$H = \int_A N N^t dA \tag{34}$$

The kinetic energy

$$T = \frac{1}{2} \int_A [R_1(\dot{u}^2 + \dot{v}^2 + \dot{w}^2) + 2R_2(\dot{u}\dot{\theta}_y - \dot{v}\dot{\theta}_x) + R_3(\dot{\theta}_x^2 + \dot{\theta}_y^2)] dA \tag{35}$$

The consistent mass matrix formulation is as follows from Eqs (33,34):

$$M = \begin{pmatrix} R_1 H & 0 & 0 & 0 & R_2 H \\ 0 & R_1 H & 0 & -R_2 H & 0 \\ 0 & 0 & R_1 H & 0 & 0 \\ 0 & -R_2 H & 0 & R_3 H & 0 \\ R_2 H & 0 & 0 & 0 & R_3 H \end{pmatrix} \tag{36}$$

Assuming a constant Jacobian determinant the above equation reduces to

$$H = \frac{A}{36} \begin{pmatrix} 4 & 2 & 1 & 2 \\ 2 & 4 & 2 & 1 \\ 1 & 2 & 4 & 2 \\ 2 & 1 & 2 & 4 \end{pmatrix} \tag{37}$$

Consistent Mass via the Projection Method

The kinetic energy of the hourglass modes is relatively large compared with the hourglass stiffness used for stabilization. Hence the mass matrix is formulated as follows, considering the kinetic energy associated with the in displacement u :

$$T_u = \int_A \frac{1}{2} R_1 \dot{u}^2 dA \qquad (38)$$

We have to eliminate the kinetic energy associated with that part of the velocity field which is ignored by the single point integration of the element stiffness, and then, expand the velocity field $\dot{u}(x,y)$ about $x = y = 0$. Hence

$$\dot{u}(x,y) = \dot{u}(0,0) + x\dot{u}_{,x}(x,y) + y\dot{u}_{,y}(x,y) + \ldots \qquad (39.a)$$

or

$$\dot{u}(x,y) = \frac{1}{4}s^t\dot{u} + x(b_1{}^t\dot{u}) + y(b_2{}^t\dot{u}) + \eta\xi(\gamma^t\dot{u}) \qquad (39.b)$$

Modifying the kinetic energy based on the purely linear part of the velocity field, that is, keeping only the linear terms from Eq (39.b)

$$\dot{u}_l(x,y) = \frac{1}{4}s^t\dot{u} + x(b_1{}^t\dot{u}) + y(b_2{}^t\dot{u}) \qquad (40)$$

gives

$$T_l = \frac{1}{2}\dot{u}^2 \left[\int_A R_1(\frac{1}{4}s + xb_1 + yb_2)(\frac{1}{4}s + xb_1 + yb_2)^t \, dA \right]\dot{u} \qquad (41)$$

As with the stiffness computation , the jacobian determinant is a constant

$$\int_A N dA = \int_{-1}^{1}\int_{-1}^{1} \frac{1}{4}(s + \xi\xi + \eta\eta + h\xi\eta)d\eta d\xi = |J|s \qquad (42)$$

31

If the center of the element is $x = y = 0$ then

$$\int_A \mathbf{x} dA = \int_A \mathbf{N}^t \mathbf{x} dA = |\mathbf{J}|(\mathbf{s}^t \mathbf{x}) = 0 \tag{43}$$

and hence terms linear in x or y do not survive the integration.

$$\int_A \mathbf{x}^2 dA = \mathbf{x}^t \mathbf{H} \mathbf{x} = c_{xx} \tag{44.a}$$

$$\int_A \mathbf{y}^2 dA = \mathbf{y}^t \mathbf{H} \mathbf{y} = c_{yy} \tag{44.b}$$

$$\int_A \mathbf{x} \mathbf{y}^2 dA = \mathbf{x}^t \mathbf{H} \mathbf{y} = c_{xy} \tag{44.c}$$

Therefore the kinetic energy

$$T_l = \frac{1}{2} R_1 \dot{u}^t \tilde{H} \dot{u} \tag{45}$$

in which

$$\tilde{H} = \frac{\mathbf{A}}{16} \mathbf{s} \mathbf{s}^t + c_{xx} \mathbf{b}_1 \mathbf{b}_1{}^t + c_{yy} \mathbf{b}_2 \mathbf{b}_2{}^t + c_{xy} (\mathbf{b}_1 \mathbf{b}_2{}^t + \mathbf{b}_2 \mathbf{b}_1{}^t) \tag{46}$$

by performing a similar linearization of all displacements and rotation components, H is replaced by $\tilde{H}$. It is evident that the kinetic energy associated with all the five hourglass modes is identically zero. And hence modes consisting primarily of hourglass motions should not appear as spurious low-energy vibration modes. The mass matrix obtained by projection onto a linearized velocity field is positive semi-definite, since zero kinetic energy is associated with all pure hourglass patterns. This mass formulation is valid for plate bending alone, since the singular modes of the mass matrix coincide precisely with those of the stiffness. The projected mass matrix yields the proper energy for all eight elementary states and zero for the hourglass modes. The mass obtained by single point quadrature leads to a proper energy only for the translational rigid body modes. Based on this, a single

32

point quadrature is used for inplane motions, and the projection method for the transverse displacements and rotations.

$$M_{opt} = \begin{pmatrix} R_1 H(1) & 0 & 0 & 0 & R_2 \tilde{H} \\ 0 & R_1 H(1) & 0 & -R_2 \tilde{H} & 0 \\ 0 & 0 & R_1 \tilde{H} & 0 & 0 \\ 0 & -R_2 \tilde{H} & 0 & R_3 \tilde{H} & 0 \\ R_2 \tilde{H} & 0 & 0 & 0 & R_3 \tilde{H} \end{pmatrix} \qquad (47)$$

where the element is sampled at the element centroid, $N = \frac{1}{4}s$. Therefore,

$$H_{(1)} = \frac{A}{16} s s^t \qquad (48.a)$$

$$= \frac{A}{16} \begin{pmatrix} 1 & 1 & 1 & 1 \\ 1 & 1 & 1 & 1 \\ 1 & 1 & 1 & 1 \\ 1 & 1 & 1 & 1 \end{pmatrix} \qquad (48.b)$$

The semi property of the single-point-integrated mass and the projection mass matrix appears to present a potential source of difficulty in some methods of eigenvalue extraction, such as subspace iteration. But the subspace projection of the mass will remain positive definite unless one or more trial vectors correspond precisely to a global deformation mode which is free of kinetic energy. This situation is highly unlikely.
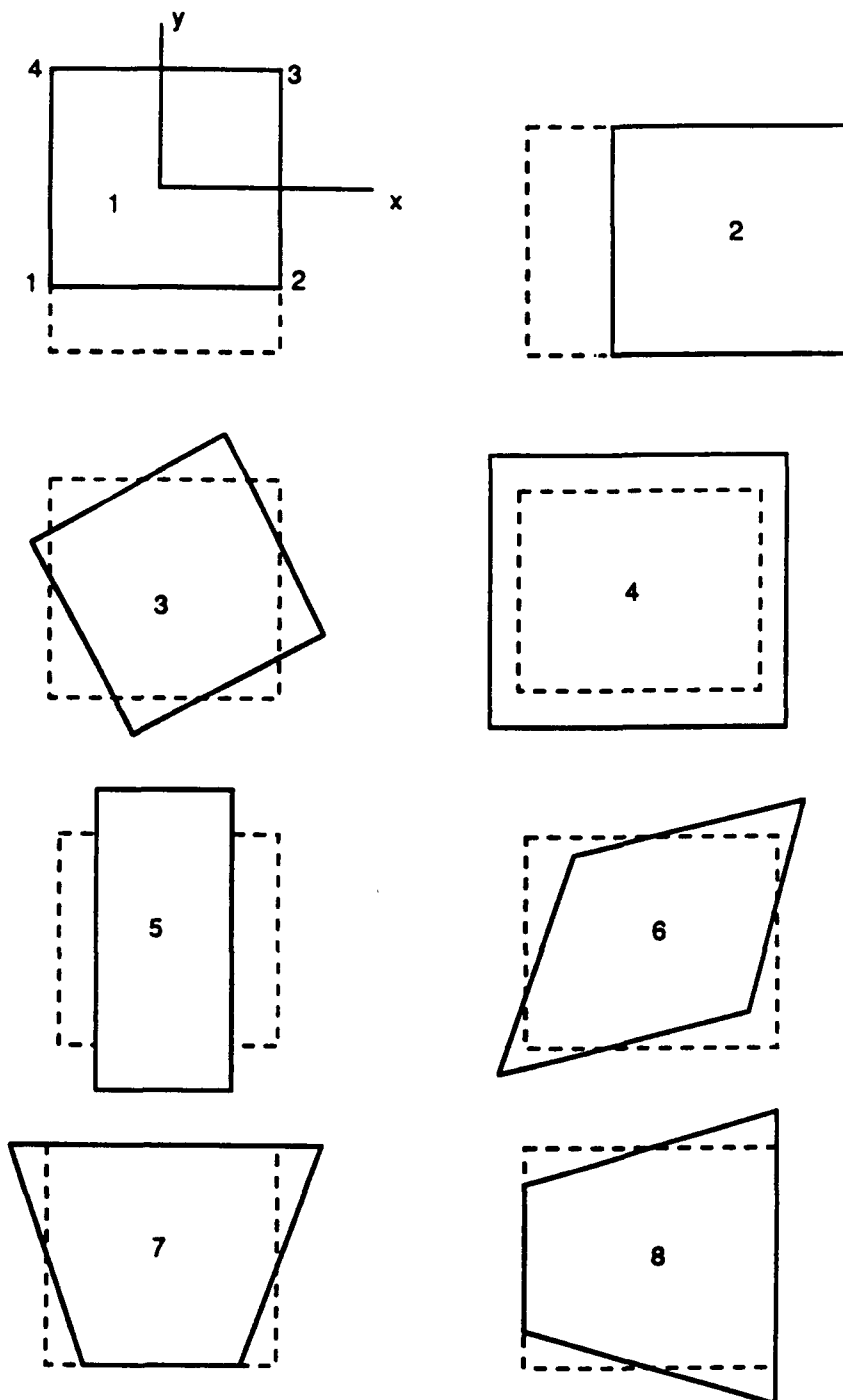
Fig. 2.1 Independent displacement modes of a bilinear element

SECTION 3

SENSITIVITY ANALYSIS

This section describes the calculations of sensitivity information for the system by the direct method. The sensitivity parameter of interest is the thickness of the plate. The optimization of structures under static loading typically requires derivatives of displacement or stress constraints. Because element stresses may be easily written as explicit functions of the nodal displacements, a general form of the constraint is

$$g(\mathbf{u}, t) \geq 0 \qquad (49)$$

In Eq (49) u is the displacement vector and t is the design variable. The derivative of g with respect to the design variable t may be written as

$$\frac{dg}{dt} = \frac{\partial g}{\partial t} + Z^T \frac{d\mathbf{u}}{dt} \qquad (50)$$

where Z is a vector such that $\frac{\partial g}{\partial u_i}$.

The first term in Eq (50) is usually zero or very easy to obtain, so the computation of the second term is discussed below.

3.1 Displacement Constraints

The static equilibrium for the structure is

$$[K]U = P \qquad (51)$$

where K is the global stiffness matrix and P is the load vector. Differentiating Eq (51) with respect to the design variable t we get

$$\frac{\partial U}{\partial t} = K^{-1}\left(\frac{\partial P}{\partial t} - \frac{\partial K}{\partial t}U\right) \qquad (52.a)$$

For load P not varying with thickness the above equation becomes

$$\frac{\partial U}{\partial t} = K^{-1}\left(-\frac{\partial K}{\partial t}U\right) \qquad (52.b)$$

Premultiplying Eq (52.b) by Z^T we obtain

$$Z^T\frac{\partial U}{\partial t} = Z^T K^{-1}\left(-\frac{\partial K}{\partial t}U\right) \qquad (52.c)$$

This above equation is solved once for each design variable. Let

$$\frac{-\partial K}{\partial t}U = -K'U \qquad (53)$$

we know

$$K = B^T D B \qquad (54)$$

therefore

$$K' = B^T D' B \qquad (55)$$

as only the D matrix contains t. Therefore

$$K'U = B^T D' B U \qquad (56)$$

36

or

$$K' U = B^T \bar{\sigma} \tag{57}$$

where

$$\bar{\sigma} = A \begin{pmatrix} \dfrac{N_x}{t} \\ \dfrac{N_y}{t} \\ \dfrac{N_{xy}}{t} \\ 3\dfrac{M_x}{t} \\ 3\dfrac{M_y}{t} \\ 3\dfrac{M_{xy}}{t} \\ \dfrac{Q_x}{t} \\ \dfrac{Q_y}{t} \end{pmatrix} \tag{58}$$

3.2 Stress Constraints

Once the solution for U' is complete from Eq (52.c) the stress sensitivities can be obtained from the following sequence. The stress derivative is derived element by element.

$$\sigma = DBU \tag{59.a}$$

$$\frac{\partial \sigma}{\partial t} = D'BU + DBU' \tag{59.b}$$

3.3 Frequency Constraints

In the natural frequency solution, the applied forces are set to zero and all the displacements are assumed to vary sinusoidally in time.

$$U = XSin(\omega t) \tag{60}$$

The resulting discrete equations of motions become:

$$KX = \lambda MX \tag{61}$$

where $\lambda = \omega^2$. This symmetric generalized eigenvalue problem is solved using the subspace iteration algorithm.

Mass matrix sensitivity calculations, as required in the sensitivity analysis of natural frequencies, are simple in form.

We have

$$KU = \omega^2 MU \tag{62}$$

The Rayleigh quotient gives

$$\omega_j{}^2 = \frac{U_j{}^T K U_j}{U_j{}^T M U_j} \tag{63}$$

where j = eigenvalue and U_j is the jth eigenvalue mode.

Differentiating

$$2\omega_j \frac{\partial \omega_j}{\partial t} = \frac{U_j{}^T M U_j{}^T (U_j{}^T K' U_j) - U_j{}^T K U_j (U_j{}^T M' U_j)}{(U_j{}^T M U_j)^2} \tag{64.a}$$

$$\frac{\partial \omega_j}{\partial t} = \frac{(U_j^T K' U_j) - \omega_j^2 (U_j^T M' U_j)}{2\omega_j U_j^T M U_j} \qquad (64.b)$$

$$= \frac{U_j^T [K' - \omega_j^2 M'] U_j}{2\omega_j (U_j^T M U_j)} \qquad (64.c)$$

for the jth mode of vibration.

The denominator is a scalar multiple of the generalized mass for the mode j, which can be calculated at the system level. The product $U_j^T K' U_j$ is calculated element by element and then assembled globally. The same is the case for the mass matrix sensitivity.

Concentrated mass added at each node will not affect the sensitivity calculation of the mass matrix, as the concentrated mass value is a constant. The total mass $M = M_s + M_c$ where M_s is the mass due to the structure and M_c is the mass due to the concentrated mass.

Differentiating

$$M' = \frac{\partial M}{\partial t} = \frac{\partial [M_s + M_c]}{\partial t} \qquad (65.a)$$

$$= \frac{\partial [M_s]}{\partial t} + \frac{\partial [M_c]}{\partial t} \qquad (65.b)$$

where

$$\frac{\partial [M_c]}{\partial t} = 0 \qquad (65.c)$$

Hence the concentrated mass does not have any affect on the mass sensitivity. Mass M is denoted as

$$M = \int_V R N N^T |J| dV \qquad (66)$$

39

were R is a function of the element density and thickness . As R is a constant for an element, it can be taken out of the integral. The element mass matrix can be differentiated with respect to the thickness easily.

Typical procedures for system level solution are outlined, assuming that element-level routines are available for evaluating the vectors $K'U$ and $M'U$, and the scalar products $U^T K'U$ and $U^T M'U$ as required. For the eigenvalue problem, for each design variable and mode, the frequency sensitivity can be summed element by element.

$$\omega_j{}' = \frac{1}{2\omega_j m_j} \sum_{e=1}^{N_{el}} [U_j{}^T K'U_j - \omega_j{}^2 U_j{}^T M'U_j] \qquad (67.a)$$

$$\mathbf{m}_j = U_j{}^T M U_j \qquad (67.b)$$

(j is not summed)

SECTION 4

OPTIMIZATION ALGORITHM

This section discusses the development of the scaling algorithm and presents the algorithm for multiobjective optimization with a discussion on reliability calculations which are used for selecting the best compromise design.

The algorithm proposed is based on optimality criteria methods (Venkayya, 1986). The optimality criteria method has the potential to extend optimization to problems with thousands of variables and constraints. One of the significant elements of the optimality criteria method is the concept of scaling. Scaling implies changing the variables with the objective of reaching the constraint boundary. The design variables can be brought to the constraint boundaries either by adding differential quantities or by multiplying the variables by scale factors. The latter is called scaling. This procedure was originally proposed for constraints which could be scaled in a single step. Later it was generalized for nonlinear functions. In both cases, however, a simple scaling algorithm was used, and it was adequate for structural optimization problems. In simple scaling a dominant constraint can be identified, and scaling with this constraint generally brings the design variables into the feasible region. This is not necessarily the case in general mathematical

41

optimization problems, and a compound scaling is necessary in order to extend the scope of the optimality criteria method. Another significant element of the optimality criteria method is modification of the variable vector at the constraint boundary by directly invoking the optimality as defined by the Kuhn-Tucker conditions. The new techniques which were developed for multiobjective optimization based on scaling are discussed in Section 4.2. The following sections explicitly discuss the development of the scaling algorithm.

4.1 Development of Scaling Algorithm

The first objective of scaling is to bring all the violated constraints to the feasible region or to the constraint boundary. If all the constraints are in the feasible region, then scaling can be used to bring some of the constraints to the constraint boundary. The mathematical basis for scaling can be derived from the first order approximation of a Taylor's series (Venkayya, 1971, 1986).

4.1.1 Scale Factor Derivation for Simple Scaling

Simple scaling is done with respect to the most prominent constraint (Figure 4.1.1.1) The scaling procedure can be explained with the help of two designs represented by the two variable vectors x and $\bar{x}$. The relationship between the two variable vectors is given by

$$\bar{x} = \Lambda x \tag{68}$$

42

where Λ is a single scalar parameter which will be referred to as a scale factor. ($\Lambda > 0$). If dx is the difference vector between the two designs, then one can write

$$dx = \bar{x} - x = (\Lambda - 1)x \tag{69}$$

Also if g and $\bar{g}$ are the response quantities respectively in the two designs, then a change in response can be represented by

$$dg = \bar{g} - g \tag{70}$$

Now from the definition of the total differential (first order approximations of the Taylor's Series) the following relationship can be written

$$dg = \frac{\partial g}{\partial x_1}dx_1 + \frac{\partial g}{\partial x_2}dx_2 + ... + \frac{\partial g}{\partial x_n}dx_n \tag{71}$$

Then dg can also be written as (from Eqs 69 and 71)

$$dg = (\Lambda - 1)\sum_{i=1}^{n} N_{i1}x_i \tag{72}$$

where $N_{i1} = \frac{\partial g}{\partial x_i}$. Dividing Eq 72 by g we have,

$$\frac{dg}{g} = (\Lambda - 1)\sum_{i=1}^{n} \frac{N_{i1}x_i}{g} \tag{73}$$

An examination of Eq 73 presents two interesting cases.

Case 1:

$$\sum_{i=1}^{n} \frac{N_{i1}x_i}{g} \leq 0 \tag{74}$$

In this case a new parameter μ is defined as

$$\mu_{jN} = -\sum_{i=1}^{n} \frac{N_{i1}x_i}{g} \tag{75}$$

43

Then Eq 73 can be written as

$$\frac{dg}{g} = (1 - \Lambda)\mu_{jN} \tag{76}$$

Now the scale factor Λ can be written as

$$\Lambda = 1 - \frac{dg}{g}\frac{1}{\mu_{jN}} = 1 - b \tag{77}$$

where

$$b = \frac{1}{\mu_{jN}}\frac{dg}{g} \qquad b \ll 1 \tag{78}$$

Equation 77 can be written as

$$\frac{1}{\Lambda} = \frac{1}{1 - b} = 1 + b \tag{79}$$

by neglecting the higher order terms of b in a binomial expansion. Now $\frac{dg}{g}$ can be written as

$$\frac{dg}{g} = \frac{\mu_{jN}}{\Lambda} - \mu_{jN} \tag{80}$$

Adding 1 to both sides of Eq 80, one can write

$$\frac{g + dg}{g} = \frac{\mu_{jN}}{\Lambda} - \mu_{jN} + 1 \tag{81}$$

A new parameter, β, which will be referred to as the target response ratio, is defined as

$$\beta = \frac{\overline{g}}{g} \tag{82}$$

Then

$$\beta = \frac{\mu_{jN}}{\Lambda} - \mu_{jN} + 1 \tag{83}$$

44

Solving for the scale factor Λ

$$\Lambda = \frac{\mu_j N}{\beta + \mu_j N - 1} \tag{84}$$

This scaling technique was originally developed by Venkayya (1971), without labelling various terms as β and μ parameters. Nevertheless, the concept has been in use for the last two decades. Substituting Λ, μ and β expressions, we get

$$\Lambda = \frac{-\sum \frac{\partial g}{\partial x_i} x_i}{\bar{g} - \sum \frac{\partial g}{\partial x_i} x_i - g} \tag{85}$$

$$\bar{g} - \sum \frac{\partial g}{\partial x_i} x_i - g = -\frac{\sum \frac{\partial g}{\partial x_i} x_i}{\Lambda} \tag{86}$$

$$\bar{g} = g + \sum \frac{\partial g}{\partial x_i} x_i (1 - \frac{1}{\Lambda}) \tag{87}$$

$$\bar{g} = g + \sum \frac{\partial g}{\partial x_i} x_i \frac{(\frac{\bar{x}_i}{x_i} - 1)}{\frac{\bar{x}_i}{x_i}} \tag{88}$$

Equation 88 is the reciprocal approximation used in mathematical programming techniques, which is

$$\bar{g}(\bar{x}) = g(x) + \sum \frac{\partial g}{\partial x_i} x_i \frac{(\bar{x}_i - x_i)}{\bar{x}_i} \tag{89}$$

This is the form Schmit and Farshi presented in 1974 as the reciprocal constraint approximation, which is a very popular technique.

Case 2:

$$\sum_{i=1}^{n} \frac{N_{i1} x_i}{g} \geq 0 \tag{90}$$

Now the parameter μ_{jP} is defined as

$$\mu_{jP} = \sum_{i=1}^{n} \frac{N_{i1} x_i}{g} \tag{91}$$

Then the scale factor Λ can be written as

$$\Lambda = \frac{\beta + \mu_j P - 1}{\mu_j P} \tag{92}$$

Decoding the above equation (92) we get

$$\Lambda = \frac{\frac{\bar{g}}{g} + \frac{\sum \frac{\partial g}{\partial x_i} x_i}{g} - 1}{\frac{\sum \frac{\partial g}{\partial x_i} x_i}{g}} \tag{93}$$

$$= \frac{\bar{g} + \sum \frac{\partial g}{\partial x_i} x_i - g}{\sum \frac{\partial g}{\partial x_i} x_i} \tag{94}$$

Simplifying

$$\bar{g}(\bar{x}) = g(x) + \sum_{i=1}^{n} \frac{\partial g}{\partial x_i} x_i \left(\frac{\bar{x}_i}{x_i} - 1 \right) \tag{95.a}$$

$$= g(x) + \sum_{i=1}^{n} \frac{\partial g}{\partial x_i} (\bar{x}_i - x_i) \tag{95.b}$$

the above equation is the linear approximation used in mathematical programming techniques (Schmit and Farshi, 1974).

An examination of Eqs 84 and 92 reveals some interesting facts:

1. In Case 1 the scale factor is inversely proportional to the target response ratio, and in Case 2 it is directly proportional to β.

2. The response of the system, g, and the response, N_{i1} can be determined from an analysis of the system for a given variable vector x. The target response (or desired response) can be determined from the constraint definition. Then the target response ratio β, and the parameter μ are known. Then the scale factor Λ can be determined explicitly for any type of structure and constraints.

46

4.1.2 Compound Scaling

In compound scaling, scaling is done with respect to multiple constraints Figure 4.1.2.1. The scale factors derived from the first order approximations of a Taylor's series Eqs 84 and 92 represent an interesting generalization for nonlinear functions. A formula involving linear and nonlinear interaction was written by Venkayya (1989) in which it was stated that, when the constraint is nonlinear the scaling formula can be represented by

$$\Lambda \quad \alpha \quad (\frac{1}{\beta})^{\frac{1}{m}} \tag{96}$$

where the parameter m is a measure of nonlinearity.

The basis for generalization of the scaling algorithm can be established by examining the μ and β parameters of two simple constraint functions.

$$g_1 = \frac{c_1}{x_1} + \frac{c_2}{x_2} + ... + \frac{c_n}{x_n} \leq \overline{g_1} \tag{97}$$

$$g_2 = c_1 x_1 + c_2 x_2 + ... + c_n x_n \leq \overline{g_2} \tag{98}$$

where $x_1, x_2, ..., x_n$ are the variables and $c_1, c_2, ..., c_n$ are a set of positive constants. The μ parameters in these two cases are defined as

$$\mu_{1N} = -\sum_{i=1}^{n} \frac{N_{i1} x_i}{g_1} = 1 \tag{99}$$

$$\mu_{2P} = \sum_{i=1}^{n} \frac{N_{i2} x_i}{g_2} = 1 \tag{100}$$

The measure of nonlinearity in both cases is 1, and it represents the linear case. The parameters β are defined as

$$\beta_1 = \frac{\overline{g_1}}{g_1} \tag{101}$$

47

$$\beta_2 = \frac{\overline{g_2}}{g_2} \tag{102}$$

It is easy to show that the exact scale factors in these two cases are simply

$$\Lambda_{1N} = \frac{1}{\beta_1} \tag{103}$$

$$\Lambda_{2P} = \beta_2 \tag{104}$$

The first condition represents Case 1, and the second represents Case 2 in the simple scaling technique discussed earlier. A similar examination was made of two nonlinear functions

$$g_1 = \frac{c_1}{x_1{}^m} + \frac{c_2}{x_2{}^m} + \dots + \frac{c_n}{x_n{}^m} \leq \overline{g_1} \tag{105}$$

$$g_2 = c_1 x_1{}^m + c_2 x_2{}^m + \dots + c_n x_n{}^m \leq \overline{g_2} \tag{106}$$

The μ parameters for these two cases are

$$\mu_{1N} = m \tag{107}$$

$$\mu_{2P} = m \tag{108}$$

The measure of nonlinearity in these two cases in m. It is easy to again show that the exact scale factors for these two cases are

$$\Lambda_{1N} = \left(\frac{1}{\beta_1}\right)^{\frac{1}{\mu_{1N}}} \tag{109}$$

$$\Lambda_{2P} = (\beta_2)^{\frac{1}{\mu_{2P}}} \tag{110}$$

For constraints with both linear and nonlinear terms it can be shown that

$$1 \leq \mu \leq m \tag{111}$$

48

The scale factors given in equation 109 and 110 are far superior approximations than those given in Eqs 84 and 92. However, they are not exact when the summation in the μ parameter definition contains both positive and negative terms. In such cases two scale factors are defined for each constraint. These correspond to Case 1 and Case 2 discussed earlier. For example, the two scale factors for the jth constraint can be defined as

$$\Lambda_{jN} = (\frac{1}{\beta_j})^{\frac{1}{\mu_{jN}}} \tag{112}$$

$$\Lambda_{jP} = (\beta_j)^{\frac{1}{\mu_{jP}}} \tag{113}$$

The definition of μ_{jN} and μ_{jP} in Eq 112 and 113 is as follows:

$$\mu_{jN} = -\sum_{i=1}^{n} \frac{N_{ij} x_i}{g_j} \tag{114}$$

and

$$\mu_{jP} = \sum_{i=1}^{n} \frac{N_{ij} x_i}{g_j} \tag{115}$$

where Eq 114 contains only negative terms and Eq 115 contains only positive terms.

4.1.3 Constraint Approximations

The conservative approximation used the above concept in building the approximate function. The constraint approximation is defined as (Starnes and Haftka, 1979)

$$\bar{g}_j = g_j + (\Lambda_j - 1)\sum_{i=1}^{n} N_{ij}x_i G_j \tag{116}$$

where

$$G_j = \frac{1}{\Lambda_{jN}} \qquad N_{ij}x_i \leq 0 \tag{117.a}$$

$$G_j = 1 \qquad N_{ij}x_i > 0 \tag{117.b}$$

Dividing Eq 116 by g_j

$$\frac{\bar{g}_j}{g_j} = 1 + (\Lambda_j - 1)\sum_{i=1}^{n} \frac{N_{ij}x_i}{g_j} G_j \tag{118.a}$$

$$\beta = 1 + (\Lambda_j - 1)\mu_j G_j \tag{118.b}$$

If μ_j is positive, then it becomes μ_{jP} and G_j becomes 1. Therefore

$$\beta = 1 + (\Lambda_{jP} - 1)\mu_{jP} \tag{119.a}$$

and

$$\Lambda_{jP} = \frac{\beta + \mu_{jP} - 1}{\mu_{jP}} \tag{119.b}$$

which is the same as the general equation derived for nonlinear constraints given in Eq 113 (when μ_{jP} is equal to 1). If μ_j is negative, then it becomes μ_{jN} and G_j becomes $\frac{1}{\Lambda_{jN}}$. Therefore

$$\beta = 1 + (\Lambda_{jN} - 1)(-\mu_{jN})(\frac{1}{\Lambda_{jN}}) \tag{120.a}$$

and

$$\Lambda_{jN} = \frac{\mu_{jN}}{\beta + \mu_{jN} - 1} \tag{120.b}$$

which is the same as Eq 112 (μ_{jN} is equal to 1).

4.2 Mutiobjective Compound Scaling (MCS) Algorithm

Multiobjective optimization was solved by modifying the generalized compound scaling algorithm (Venkayya, 1991) for multiobjective optimization problems. This technique generates a partial Pareto optimal set. For a multiobjective problem there exists several Pareto optima. Since the determination of all the Pareto optima of a multiobjective problem is computationally expensive, a subset of the Pareto optimal points is sufficient for finding the solution. As stated by Rao (1988) and observed by many other researchers the optimum solution generated by the various multicriteria optimization methods can be different from each other, hence a solution concept or procedure should be defined on the basis of other attributes such as the mathematical basis of the method, its generality and the quality of the final solution. Keeping this in mind the generalized compound scaling algorithm for multiobjective or vector optimization is built.

The MCS algorithm is based on scaling techniques. The basic idea of any scaling algorithm being to derive a set of scale factors for the variables such that the design can be brought to the constraint surface in one or more steps from anywhere in the n-dimensional design space by multiplying the current values of the variables and the scale factors. The implication being that the optimum lies on the constraints surface or intersection of the constraints. To generalize the scaling technique the objective functions are also treated as additional constraints, as both the constraints and the objective function are functions of the same variables. In multiobjective optimization it is well known that the Pareto optimal set lies on the intersection of the objective functions contours, hence treating the objective functions in the same

51

way as the constraints seems a logical approach. So once an optimum constraint surface or intersection of constraint surfaces is reached, the MCS technique tries to reduce one of the objective functions depending on the objective function gradient information. The difficulty in treating the objective functions as constraints is that the constraints have a target to satisfy and the objective functions do not. Hence to make the objective functions look like constraints, pseudo target values for the objective functions are generated so that they can be treated as additional constraints which intersect other constraints. Linear as well as nonlinear objective functions were considered to demonstrate the robustness of the algorithm.

Multicriteria Problem

The problem of multiobjective optimization subject to multiple constraints can be posed as:

Minimize

$$F = [F_1(\mathbf{x}), F_2(\mathbf{x}), ..., F_q(\mathbf{x})] \qquad (121)$$

subject to the constraints

$$g_j(x_1, x_2, ..., x_n) \le \bar{g}_j \qquad j = 1, 2, ..., o. \qquad (122.a)$$

$$g_j(x_1, x_2, ..., x_n) = \bar{g}_j \qquad j = o + 1, ..., m. \qquad (122.b)$$

and the side bounds on the design variables as

$$x_i \ge x_i^{(l)} \qquad i = 1, 2, ..., n. \qquad (123)$$

where F are the conflicting objectives to be minimized, q is the total number of objectives, n is the number of design variables and m is the total number of constraints.

MCS Algorithm

The technique makes use of the active set constraint strategy hence reducing the computational effort considerably (Venkayya and Tischler, 1989). The two most important parameters are the target response ratio and the characteristic function. They are denoted by β and μ, respectively. In general, to put it in a broad sense, the $\beta's$ are the scale factors magnitudes for the new design vector, and the $\mu's$ are the direction vectors for the magnitudes. The Figure showing the sequence of operations is given in Figure 4.2.1.

First, β (target response ratio) parameters are computed for all the constraints using the following expression (same as Eq 82).

$$\beta_i = \frac{\overline{g}_i}{g_i} \qquad i = 1, 2, ..., m \tag{124}$$

If g_i and $\overline{g}_i$ are positive, then the following statements are valid. $\beta_i = 1$ represents the constraint surface, $\beta_i > 1$ represents the feasible region, and $\beta_i < 1$ represents the infeasible region.

After arranging the constraints with the β's in ascending order, the constraints with the lowest β values being the most critical are selected for the active constraint set (about 10 to 15) and denoted by s. Next, the characteristic function parameter

53

μ is computed for each of the selected s constraints and the objective functions. The μ parameter consists of two parts based on the sign of the individual terms in the summation. This basically stores the gradient information of the constraints and the objective function.

For all negative μ_{ij} terms

$$\mu_{jN} = -\sum_{i=1}^{n} \mu_{ij} \qquad j = 1, 2, ..., s + q \qquad (125.a)$$

For all positive μ_{ij} terms

$$\mu_{jP} = \sum_{i=1}^{n} \mu_{ij} \qquad j = 1, 2, ..., s + q \qquad (125.b)$$

where

$$\mu_{ij} = \frac{N_{ij} x_i}{z_j} \qquad j = 1, 2, ..., s + q \qquad (125.c)$$

where z_j is a vector containing the values of s selected constraints and the q objective functions. N_{ij} is the ordered gradient matrix corresponding to the selected active constraint set s in the order of their β values which are sorted in ascending order and derivatives of the objective functions with respect to the design variables.

To make the objective functions look like constraints, one may write

$$F_i(x) \le \overline{F_i} \qquad i = 1, 2, ..., q$$

where $\overline{F_i}$ are pseudo targets for the objective functions. Two distinct cases are identified for assigning the β values for the objective functions.

Case 1:

When the design is away from the constraint surface,

then

$$\delta = \frac{1 + \alpha\beta_1}{1 + \alpha} \tag{126.a}$$

$$\beta_k = \delta \qquad \mu_{kN} \geq \mu_{kP} \tag{126.b}$$

$$\beta_k = \frac{1}{\delta} \qquad \mu_{kN} < \mu_{kP} \tag{126.c}$$

where $k = s+1, s+2, ...q$, and β_1 is the target response ratio for the most violated or most active constraint from the active constraint set s. The α is calculated using the information provided from the corresponding characteristic function μ for the same selected constraint.

$$\gamma = \frac{1}{\mu_1} \tag{127.a}$$

$$\alpha = \gamma \qquad \mu_{1N} \geq \mu_{1P} \tag{127.b}$$

$$\alpha = \frac{1}{\gamma} \qquad \mu_{1N} < \mu_{1P} \tag{127.c}$$

where μ_1 is the larger value of the positive (μ_{1P}) or negative (μ_{1A}) for the selected constraint.

Case 2:

In the second case when the design is on the constraint boundary, the β parameter of the objective functions are weighed, and the objective function which has the smallest β value is selected for scaling down. Then the objective function selected is scaled down by multiplying or dividing the current values of the variables

by a factor depending on whether the gradient of the objective function is positive or negative with respect to that variable. The value of the factor is generally taken as 0.8.

The next step is to calculate the scale factors. Scale factors Λ depend on the values of the function characteristic parameters and target response ratios. The procedure is as follows:

$$\Lambda_{jN} = (\frac{1}{\beta_j})^{\frac{1}{\mu_{jN}}} \qquad \mu_{jN} \geq \mu_{jP} \qquad (128.a)$$

or

$$\Lambda_{jP} = (\beta_j)^{\frac{1}{\mu_{jP}}} \qquad \mu_{jN} < \mu_{jP} \qquad (128.b)$$

The following conditions are used in constructing the scale factors matrix.

$$\left.\begin{array}{ll} \Lambda_{ij} = \Lambda_{jN} & \mu_{ij} < 0 \\ \Lambda_{ij} = 1.0 & \mu_{ij} \geq 0 \end{array}\right\} \ \mu_{jN} \geq \mu_{jP} \qquad (129.a)$$

or

$$\left.\begin{array}{ll} \Lambda_{ij} = \Lambda_{jP} & \mu_{ij} > 0 \\ \Lambda_{ij} = 1.0 & \mu_{ij} \leq 0 \end{array}\right\} \ \mu_{jN} < \mu_{jP} \qquad (129.b)$$

This results in $s + q$ possible scale factors for each variable. The strategy in compound scaling is to select a mix of the scale factors from various columns of the scale factor table with the object of approaching the intersecting points of the constraints. The relevant scale factors are determined with the help of a scale factor assignment procedure. The underlying concept is similar to pivoting for identifying prominent variables. The scale factors assignment table is computed as follows

$$\left.\begin{array}{ll} t_{ij} = |\frac{N_{ij}z_i}{z_j}| \div \mu_{jN} & \mu_{ij} < 0 \\ t_{ij} = 0 & \mu_{ij} \geq 0 \end{array}\right\} \ \mu_{jN} \geq \mu_{jP} \qquad (130.a)$$

56

or

$$t_{ij} = \left|\frac{N_{ij}z_i}{z_j}\right| \div \mu_j P \qquad \mu_{ij} > 0 \\ t_{ij} = 0 \qquad\qquad \mu_{ij} \leq 0 \Bigg\} \qquad \mu_j N < \mu_j P \qquad (130.b)$$

The values of the entries in the scale factor assignment table vary from zero to one.
Now all the information is available for the selection of an appropriate scale factor
for each variable from the list of $s + q$ scale factors. The appropriate scale factor
for the ith variable is selected based on the following principles:

(i) From the scale factor assignment matrix select the largest entry in the ith row.

For Example: If t_{ij} is the largest entry in the scale factor assignment matrix,
then the appropriate scale factor for the ith variable is the Λ_{ij} from the scale factor
matrix.

(ii) If there is more than one entry equal to the largest entry in that row, then
the appropriate scale factor corresponds to the smallest β_j of the equal entries.
Now this process of selecting the appropriate scale factor is applied to all the
variables. The selected scale factor for the ith variable is denoted by r_i. The
scaled variables for x_i are computed by

$$x_i^{new} = r_i x_i^{old} \qquad i = 1, 2 \ldots n \qquad (131)$$

The compound scaling algorithm simply drives the design to the intersection of
the constraints, if such an intersection exists. This can be illustrated well with an
example which consists of two design variables and two constraints for a bicriteria
optimization problem. The problem statement is as follows:

57

Demonstration Problem

Minimize

$$F_1 = 4x_1 + x_2 \tag{132.a}$$

$$F_2 = \frac{0.004}{x_2 + 0.25x_1}. \tag{132.b}$$

Subject to

$$g_1 = \frac{1.6}{x_2 + 0.25x_1} \leq 1.0 \tag{133.a}$$

$$g_2 = 0.2\left[\frac{\sqrt{3}}{3x_1} + \frac{2}{x_2 + 0.25x_1}\right] \leq 1.0 \tag{133.b}$$

Start with an initial design $x_0 = (0.1, 1.0)$ which are the lower bounds of the design variables. It can be seen from Figure 4.2.2 that in one scaling the design reaches the intersection of the two constraints g_1 and g_2. This comes about because of the resultant vector direction of the gradients of the two constraints, and the scale factor is calculated as discussed above. At point A in Figure 4.2.2 it can be seen that moving in the direction of objective function F_1 for minimization will violate the constraints. Hence at point A the designs are scaled by a factor 0.8 with respect to F_2 depending on the gradients of the second objective function. This is point B in Figure 4.2.3. From point B the design moves to the intersection of g_1, F_1, F_2 to point C shown in Figure 4.2.3. The dark highlighted curve shows the minimal curve (Pareto optimum). In this procedure the design moves into the feasible region and then back to the constraint boundary.

4.3 Reliability Criteria

In multiobjective optimization there are a number of Pareto optimal design:
which can be picked as an acceptable and "valid" design. Most decisions on the
choice of the "best" or "suitable" design are based on preferential decision making
where the decision maker already has set priorities in the objective functions. One
possible approach for selection of a "suitable" design could be done by probabilistic
methods. A reliability based procedure has definite advantages over a deterministic
design procedure.

A general approach for estimating the variance of structural response variables,
given the mean values and variances of system properties which are probabilistic
in nature, is outlined. Here the probabilistic properties of a system are viewed as
discrete random variables. The thickness of a plate or any design variable may vary
due to manufacturability or some other criteria, and hence can be characterized by
a mean value and a single value of the variance.

The statistical parameter of interest in the present work are the thicknesses of
the plates which are the design variables of the structure. The structural response
quantities that we are interested in are displacement, stress, and natural frequency.
The results from these calculations can be interpreted in may different ways. One
of the most important being that the variance calculations generate a single scalar
quantity for each of the different parameters such as displacement at a location of
interest, stress at a critical region or system natural frequency. This makes it easier
in judging the behavior of the structure to the variance in the design variables.

In the optimization problem the constraint function, $g_i(X)$, represents each mode of malfunction or failure of the system. For given values of random variables this function separates the space of random variables into safe and failure zones. That is

$$g_i(X) > 0 \rightarrow \textbf{safe} - \textbf{space} \qquad (134.a)$$

$$g_i(X) < 0 \rightarrow \textbf{failure} - \textbf{space} \qquad (134.b)$$

where the boundary between these two regions, $g_i(X) = 0$, is called a failure surface or limit state function. If the joint probability density function of the random variables, $f_X(x)$, is known, then the reliability measure associated with the ith constraint can be obtained as follows (Rao, 1984):

$$P_{si} = \int_{g_i > 0} f_X(x) dx \qquad (135)$$

As the joint distribution of the random variables is rarely known and also the integral evaluation is extremely difficult, approximations for the above integral have been proposed by many researchers. Approximating Eq 135, the probability is calculated as

$$P_{si} = \phi(\eta_i) \qquad (136)$$

where $\phi(\cdot)$ is the standard normal probability distribution function, and η_i is the reliability index for the ith failure mode defined as

$$\eta_i = \frac{\bar{g}_i(X)}{\sigma(g_i)} \qquad (137)$$

$\bar{g}_i(X)$ is the mean value of the constraint, and $\sigma(g_i)$ is the standard deviation. These are calculated as shown below;

$$\bar{g}_i(X) = g_i(\bar{X}) \qquad (138)$$

$$\sigma_{g_j} = [\sum_{i=1}^{n}(\frac{\partial g_j}{\partial x_i})_{\bar{X}}^2 \sigma_{x_i}^2]^{\frac{1}{2}} \tag{139}$$

where n denotes the total number of design variables. The method for evaluating η_i, by expanding around the mean value of the random variables, is known as a first-order second moment method (Nikolaidis and Burdisso, 1988).

For limit state functions that are not highly nonlinear, the probability of failure can be approximated with good accuracy as

$$P_{f_i} = \phi(-\eta_i) \tag{140.a}$$

or

$$P_{f_i} = 1 - P_{s_i} \tag{140.b}$$

The individual failure probabilities of each failure subsystem were combined to evaluate the system probability of failure. The exact evaluation of the failure probability is a formidable task that requires knowledge of the joint probabilities corresponding to all combinations of the failure modes.

Approximating the system failure probability by various bounds that can be evaluated inexpensively, Ditlevsen's first order upper bound is selected for calculating system reliability (Yang and Nikolaidis, 1990). This is because in this formulation the failure modes are completely independent, and the approximation is valid for the range of values of P_f usually encountered in structural optimization applications (Davidson, et.al, 1977). System probability can be defined as

$$P_s = \Pi_{i=1}^{m}(1 - P_{f_i}) \tag{141.a}$$

61

If the values of the P_{fi} are small, higher order terms are neglected, and the above equation can be redefined as follows:

$$P_s = 1 - \sum_{i=1}^{m} P_{fi} \qquad (141.b)$$

$$P_f = \sum_{1=1}^{m} P_{fi} \qquad (141.c)$$

where P_f is the system failure probability, P_{fi} is the probability of the individual failure mode, and m denotes the number of failure modes.

$$X_0 = \begin{vmatrix} 0.1 \\ 1.0 \end{vmatrix} \quad X_{NEW} = \Lambda \begin{vmatrix} 0.1 \\ 1.0 \end{vmatrix} = \begin{vmatrix} 0.156 \\ 1.560 \end{vmatrix} \quad \Lambda = 1.560$$

$$g_0 = \begin{vmatrix} 1.58 \\ 1.54 \end{vmatrix} \quad g_{NEW} = \begin{vmatrix} 0.997 \\ 1.070 \end{vmatrix}$$

Fig. 4.1.1.1 Graphical interpretation of simple scaling

63

$$X_0 = \begin{vmatrix} 0.1 \\ 1.0 \end{vmatrix} \quad X_{NEW} = \begin{vmatrix} 0.1\,\Lambda_1 \\ 1.0\,\Lambda_2 \end{vmatrix} = \begin{vmatrix} 0.179 \\ 1.560 \end{vmatrix} \quad \begin{matrix} \Lambda_1 = 1.79 \\ \Lambda_2 = 1.56 \end{matrix}$$

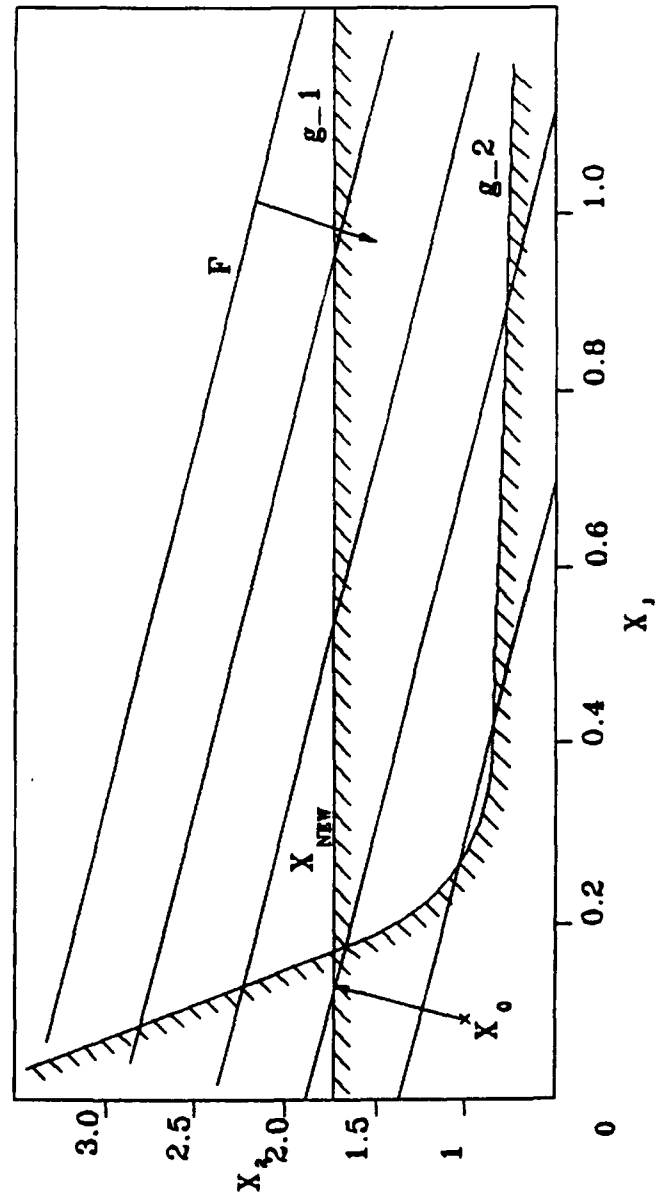$$g_0 = \begin{vmatrix} 1.56 \\ 1.54 \end{vmatrix} \quad g_{NEW} = \begin{vmatrix} 0.997 \\ 0.900 \end{vmatrix}$$
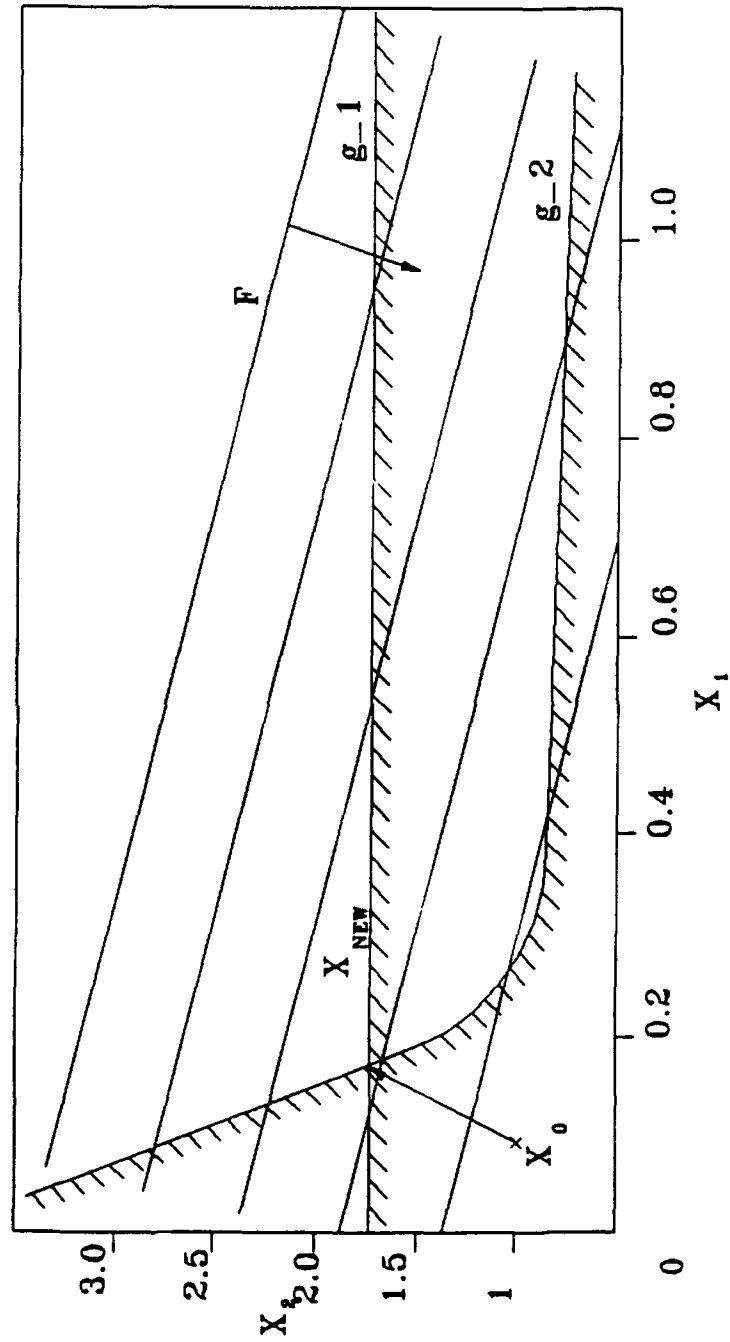
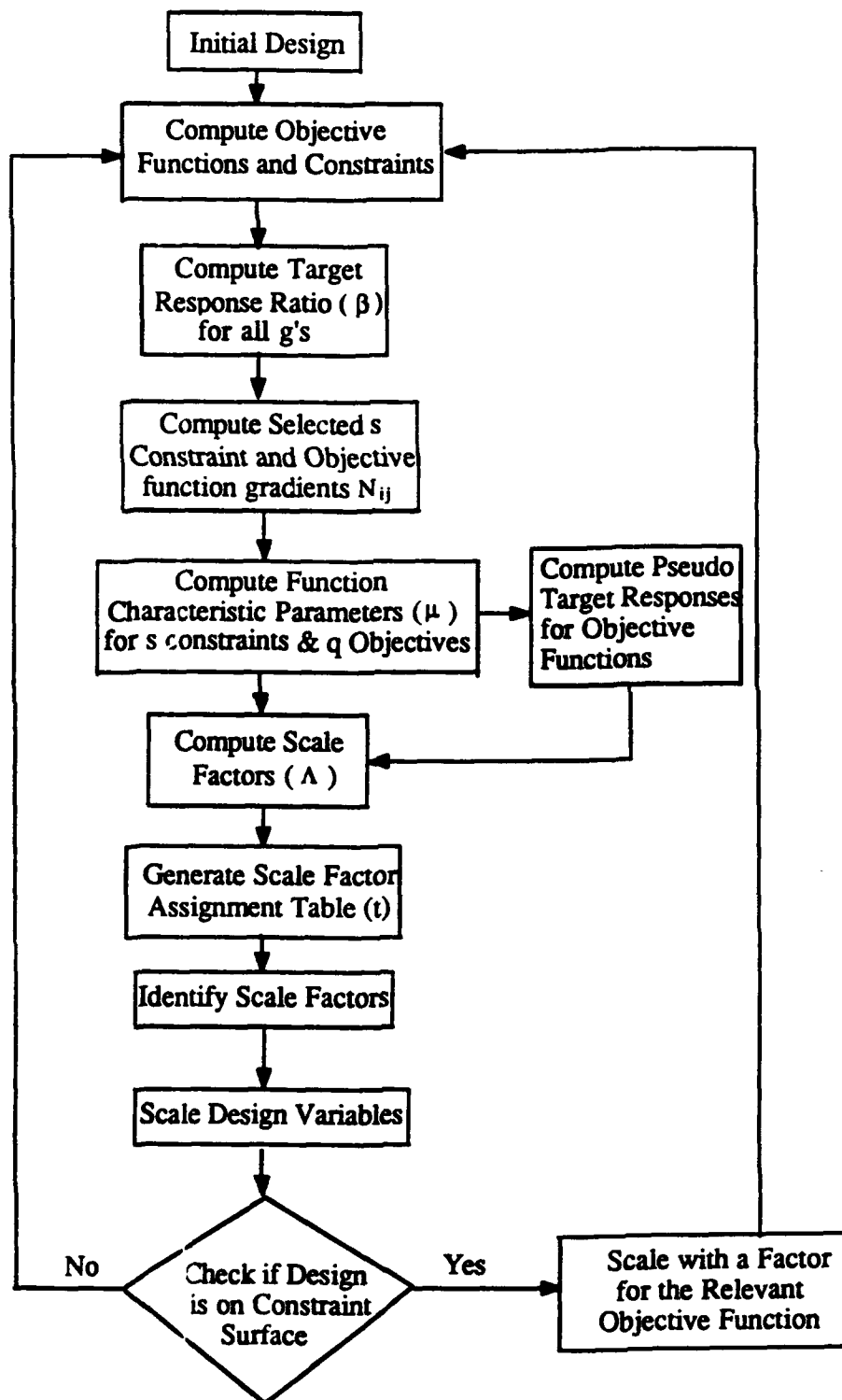Fig. 4.1.2.1   Graphical interpretation of compound scaling

64

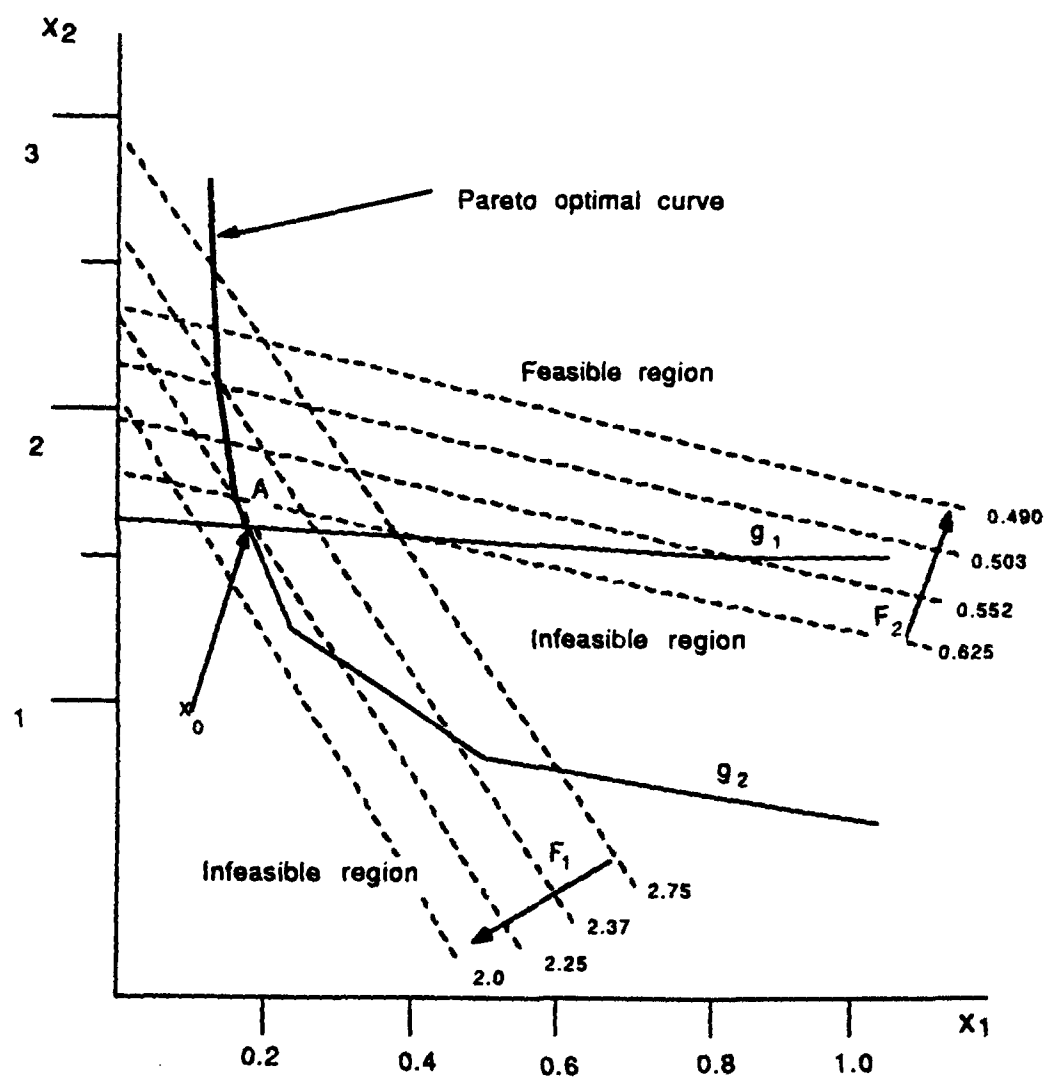Fig. 4.2.1 Multiobjective Compound Scaling (MCS)
Algorithm Flow-Chart

Fig. 4.2.2 Demonstration problem for bicriterion optimization

66
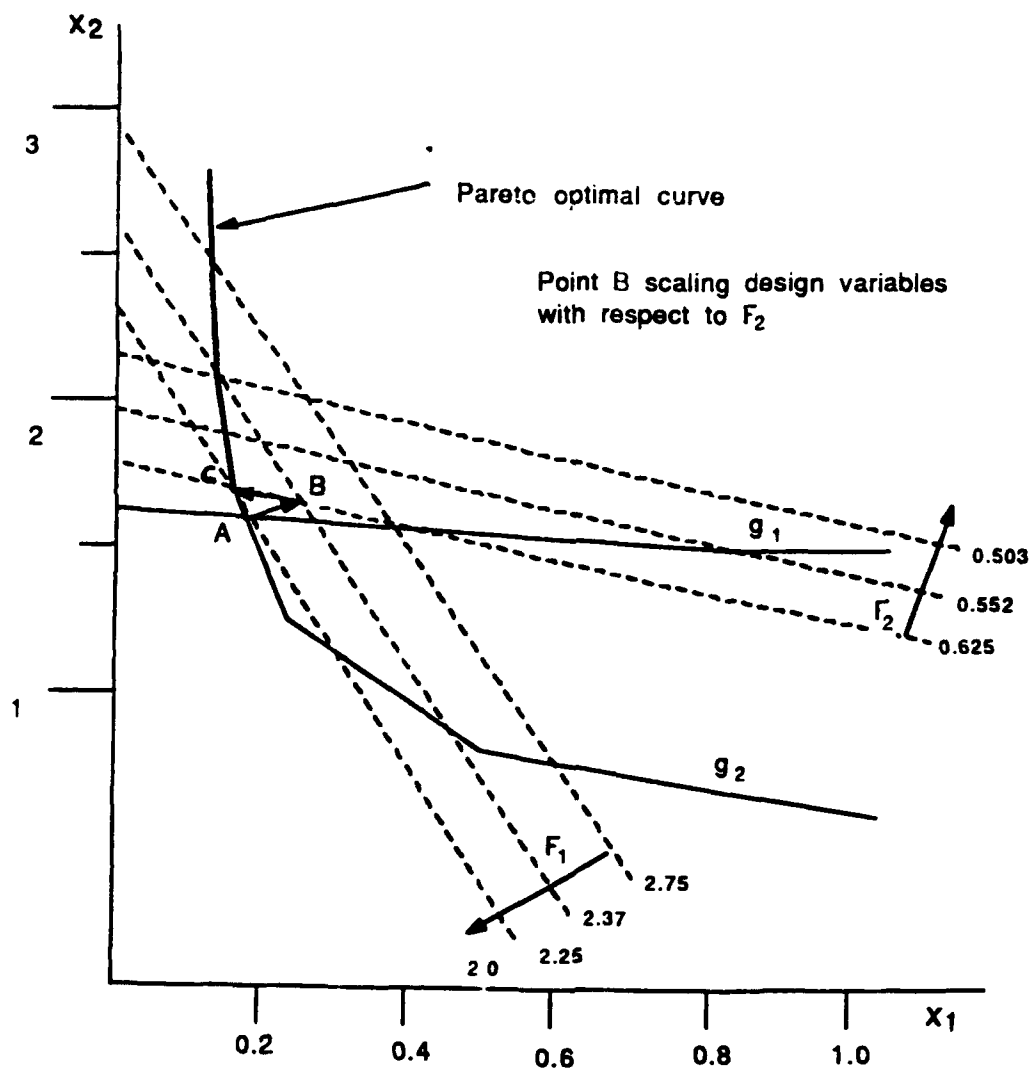
Fig. 4.2.3 Demonstration problem for bicriterion optimization

67

SECTION 5

NUMERICAL RESULTS AND DISCUSSIONS

In this section eight example problems are solved using the MCS technique.

5.1 Example 1: Two Bar Truss

The two bar truss shown in Figure 5.1.1 is considered for illustrating the MCS approach (Rao, *et.al.*, 1988). The cross sectional area of the member and the position of joints 1 and 2 are treated as the design variables. The truss is assumed to be symmetric about the y axis. The coordinates of joint 3 are held constant. The weight of the truss and the displacement of joint 3 are considered as the objective functions F_1 and F_2, respectively. The stresses induced in the members are constrained to be less than the permissible stress, σ_0. In addition, lower bounds are placed on the design variables. Thus the problem can be stated as:

Minimize

$$F_1(X) = 2\rho h x_2 \sqrt{1 + x_1{}^2} \qquad (142.a)$$

$$F_2(X) = \frac{Ph(1 + x_1{}^2)^{1.5}(1 + x_1{}^4)^{0.5}}{2\sqrt{2}E x_1{}^2 x_2} \qquad (142.b)$$

68

Subject to

$$g_1(X) = \frac{P(1 + x_1)(1 + x_1{}^2)^{0.5}}{2\sqrt{2}x_1 x_2} - \sigma_0 \leq 0 \qquad (143.a)$$

$$g_2(X) = \frac{P(x_1 - 1)(1 + x_1{}^2)^{0.5}}{2\sqrt{2}x_1 x_2} - \sigma_0 \leq 0 \qquad (143.b)$$

where $x_1 = \frac{z}{h}, x_2 = \frac{A}{A_{min}}$, E = Young's modulus, ρ = density of the material, the lower bound on the first design variable is 0.1 in, and the lower bound on the second design variable is 1.0 in. The problem data is ρ=0.283 $\frac{lb}{in^3}$, h = 100 in, A_{min} = 1 in^2, P = 10,000 lb, E = 30 × $10^6 \frac{lb}{in^2}$, σ_0 = 20,000 $\frac{lb}{in^2}$. The constraints are normalized by dividing the values with σ_0. The multicriteria optimization was performed using the generalized scaling algorithm. The MCS generates a number of optimal Pareto solutions. Which one of these designs is to be taken as the optimum is decided by calculating the reliability criteria of the system. After elimination based on reliability calculations of all the constraints, two possible designs Table 5.1.1, are obtained which need some discussion. Case 1: (iter no. 7) F_1 = 86.761 and F_2 = 0.115. This design is in the feasible region with both the constraints being inactive. Case 2: (iter no. 8) F_1 = 81.860 and F_2 = 0.041. This design also is in the feasible region with none of the constraints active. Using the system reliability information the design at iteration 8 was taken as the optimum. The corresponding optimum design variables are x_1 = 0.858 and x_2 = 1.0972. Optimum obtained by Rao are shown in comparison with the MCS results in Table 5.1.1. For this example problem MCS did not perform well in generating some of the Pareto optimal solutions, because the optima's do not lie on the constraint surface.

5.2   Example 2: Production Planning Problem

Consider a production planning problem example (Osyczka,A., 1984) in which product A is of high quality and product B is of lower quality. The profits are 4 and 5 dollars per product respectively. The best customer of the company wishes to have as many as possible of type A product. Then the two objectives, (1) the maximization of profit and (2) the maximum production of product A, should be considered. Hence, the design variables are x_1 = number of units of products A to produce and x_2 = number of units of product B to produce. Both products require time in two departments. Product A requires 1 hour in the first department and $1\frac{1}{4}$ hours in the second department. Product B requires 1 hour in the first department and $\frac{3}{4}$ in the second department. The available hours in each department are 200 monthly. Furthermore, there is a maximum market potential of 150 units for product B. These restrictions are the constraints. Hence, the optimization problem can be written as follows:

Minimize

$$F_1(X) = 1000.0 - 4x_1 - 5x_2 \qquad\qquad (144.a)$$

$$F_2(X) = 1000.0 - x_1 \qquad\qquad (144.b)$$

Subject to

$$g_1(X) = x_1 + x_2 \leq 200 \qquad\qquad (145.a)$$

$$g_2(X) = 1\frac{1}{4}x_1 + \frac{3}{4}x_2 \leq 200 \qquad\qquad (145.b)$$

$$g_3(X) = x_2 \leq 150 \qquad\qquad (145.c)$$

70

$$x_1, x_2 \geq 0 \qquad\qquad (145.d)$$

In this example as the problem is two-dimensional a graphical representation of the problem formulation is shown in Figure 5.2.1 (a). In this space the inequality constraints form a set of feasible solutions. The Pareto set for the problem is shown in Figure 5.2.1 (b), from which it can be seen that F^p are the possible Pareto solutions. The possible Pareto sets generated by the MCS are shown in Table 5.2.1. It can be seen that the Pareto solutions generated by MCS follow the dark line shown in Figure 5.2.1(b) which are the Pareto solutions for the problem. For this particular problem the MCS generated almost the complete Pareto set, because the problem was linear in nature and the Pareto solutions lie on the constraint surfaces.

5.3 Example 3 : Apartment Problem

This problem is taken from Eschenauer's *et.al.*, (1990) book. The problem is stated as: maximize floor area and minimize the construction cost. The design variables are: x_1 living room length, x_2 hall length, x_3 bedroom number three length, x_4 kitchen length, and x_5 bedroom length.

The constraints are

$$4.28x_1 \leq 30 \qquad\qquad (146.a)$$

$$4.28x_1 \geq 15 \qquad\qquad (146.b)$$

$$3.05x_4 \leq 12 \qquad\qquad (146.c)$$

$$3.05x_4 \geq 5 \qquad\qquad (146.d)$$

71

$$1.83x_2 \leq 7.2 \qquad\qquad (146.e)$$

$$2.45x_2 \leq 6.5 \qquad\qquad (146.f)$$

$$2.45x_2 \geq 4.5 \qquad\qquad (146.g)$$

$$3.05x_5 \leq 18 \qquad\qquad (146.h)$$

$$3.05x_5 \geq 10 \qquad\qquad (146.i)$$

$$3.35x_3 \leq 18 \qquad\qquad (146.j)$$

$$3.35x_3 \geq 10 \qquad\qquad (146.k)$$

$$3.98x_3 \leq 18 \qquad\qquad (146.l)$$

$$3.98x_3 \geq 10 \qquad\qquad (146.m)$$

$$x_1 + x_2 - x_4 - x_5 = 0.0 \qquad\qquad (146.n)$$

The above problem is a multicriteria linear programming formulation. Table 5.3.1 shows the Pareto-optimal solutions generated by MCS, and Figure 5.3.1 shows the Pareto solutions generated by the constraint method. From both of these we can see that MCS generated a partial Pareto-optimal set.

5.4 Example 4: Cantilever Beam with an End Moment

A beam of 10 in length and 1 in (Figure 5.4.1) wide is optimized for minimum weight and maximum first natural frequency. The material properties are: $E = 10^7 psi$, $\nu = 0.3$, $\rho = 0.1 \frac{lb}{in^3}$. The beam is subjected to an end moment of 450 $lb - in$. The allowable normal stress (σ_x, σ_y) is $\sigma_{max} = 30,000$ psi. It is required that the tip deflection be limited to 0.5 in. The lower bound on the thicknesses

was 0.1 *in.* The beam is modelled into 20 elements as a 20×1 mesh. In the initial design all the element thicknesses were 0.5 *in.* The initial weight was 0.5 *lb*, and the corresponding natural frequency was $\omega_1 = 999.08 \frac{rad}{sec}$. For the optimization problem the total number of design variables was 20 (element thickness), and the total number of constraints was 82 (42 displacements and 40 normal stresses).

The individual optimum obtained for the two objective functions are shown in the Table 5.4.1. Using the constraint method the complete Pareto set for the problem was generated. The feasible designs generated by the MCS algorithm and the Pareto set generated by the constraint method are shown in Figure (5.4.2). From the figure it can be inferred that the feasible designs generated by MCS follow quite closely to the constraint method. As the optimization progresses utilizing the sensitivity and constraint information , system reliability is calculated at each iteration. From Table(5.4.1) it can be seen that the designs which need further investigation are the ones from iteration 6, 8, 12, etc., since the reliability of the whole structure is highest at these designs. Let us consider iteration number 6. At this design the stress constraint at the tip element is active. The displacement constraint is inactive. The optimum obtained for the two criteria are $W = 0.403 lb$ and $\omega_1 = 1123.363 \frac{rad}{sec}$. For the design at iteration 8 the same constraint is active, but the displacement at the tip is lower. The optimum are $W = 0.576$ *lb* and $\omega_1 = 1885.205 \frac{rad}{sec}$. From the calculation of the reliability criteria for the system we can select the design of iteration 6 as it has a higher system reliability than the other Pareto optimal. Notice for a 9 % increase in weight a 31 % increase in ω_1 was

73

achieved. The optimal distribution for the design at iteration 6 and 8 is shown in Table. 5.4.2.

5.5 Example 5 : Square Plate Clamped at the Edges

A square plate clamped at the edges is minimized for weight and for maximum nodal displacement which for this problem happens to be at the center of the plate (node 121). The plate is subjected to a uniform lateral load of 110.3 kPa. The plate dimensions are 508 x 508 mm. The configuration is shown in Figure 5.5.1. Only a quarter of the plate is considered due to symmetry. The material properties are (Aluminum) $E = 72.4$ GPa, $\nu = 0.3$, $\rho = 2.77$ gm/cm^3. The plate was modelled with 100 elements with a mesh size of 10×10. The maximum allowable normal stress (σ_x, σ_y) was $\sigma_{max} = 82.7$ MPa. The lower bound on the design variable was 1.0 mm.

The initial weight of the structure was 1.36 kg, and the corresponding displacement (at node 121) was 3.15 mm with an uniform design of 7.62 mm. The total number of design variables was 100 (element thickness), and the total number of constraints was 200 (normal stresses in the x and y direction). No attempt was made to reduce the number of design variables by linking. The MCS technique generated a partial Pareto set with four designs which need further consideration. As the number of active constraints increases, the number of Pareto solutions decrease which can be seen in this particular problem wherein the number of stresses reaching the limit is always ten or more at any of the Pareto optimal designs. These designs are shown in Table 5.5.1. The table also shows the corresponding system reliability for

each particular design. From the table it can be seen that the design at iteration 11 has the highest reliability when compared to the others. The partial solution set produced by MCS and the constraint method are plotted in Figure 5.5.2. The constraint method shows the complete Pareto set. At the optimal design selected (selected using reliability) the thickness distribution around the center of the plate was high. Stresses at the regions about the central axis where double symmetry of the structure exists were active. The thickness distribution at the optimum is shown in Table 5.5.2. The optimum design is plotted in Figure 5.5.3.

5.6 Example 6 : Plate on Four Diagonal Supports

A rectangular steel plate of 10 $in \times$ 12 in (Figure 5.6.1) supported at four points on the diagonals is the next problem solved. The plate is loaded along the central and boundary lines of the plate. The problem is simple enough to analyze, however, because of the overhang a complex saddle deformation pattern forms around the support points (Prasad and Haftka, 1979). The material properties are Young's Modulus, $E = 28 \times 10^7 psi$, Poisson's ratio, $\nu = 0.3$ and mass density, $\rho_m = 7.71 \times 10^{-04} \frac{lbs^2}{in^4}$. The loading configuration is shown in Table 5.6.1. The finite element model consists of 49 elements (a mesh of 7 $\times$ 7) , as only one-quarter of the plate is actually modeled due to symmetry. The diagonal support point is assumed to be located at two fifths of the distance between the plate's corner and its center. A total of 6 lb of non-structural mass was added to the structure. The lower bound on the design variables was 0.02 in. The limits on displacement and stress were 0.02 in and 25000.0 psi, respectively. The initial design started from a feasible

75

point and had a weight of 12.340 *lb*. The corresponding fundamental frequency was $\omega_1 = 5400.662 \frac{rad}{sec}$, when all the design variable thicknesses were at 0.71 *in*.

The structural weight was minimized and the fundamental frequency was maximized subject to stress and displacement constraints. The total number of design variables was 49 (element thickness), and the total number of constraints was 162 (64 displacements and 98 normal stresses). Figure 5.6.2 shows the Pareto optimal set generated by the constraint method, and the partial Pareto set generated by the MCS algorithm. Table 5.6.2 gives the individual minima's and a few Pareto optimal with their respective system reliability. Going through the Pareto optimal solution the design at iteration no. 31 is selected as the best compromise design. At this design the displacement at node 8 was active, and a few stresses were active. None of the optimal thicknesses were at the lower bound. From this design it can be seen that we have achieved a good compromise design between the two individual minima's. Figure 5.6.3 gives the mode shapes corresponding to the first and second frequencies. Table 5.6.3 gives the first five frequencies at the initial and optimum designs. Table 5.6.4 gives the optimal thickness distribution. Figure 5.6.4 shows the optimal design.

5.7 Example 7: Simply Supported Square Plate

A square plate simply supported at the edges with dimensions 10 *in* × 10 *in* was optimized for minimum weight (Figure 5.7.1). The material properties are: Young's modulus, $E = 10^7 psi$, Poisson's ratio, $\nu = 0.3$ and mass density, $\rho_m = 2.587 \times 10^{-04} \frac{lbs^2}{in^4}$. A uniformly distributed load of 100 *psi* was applied. The plate was

modelled using 64 finite elements (a mesh of 8 × 8) . Double symmetry of the plate was observed about the central axes and hence only a quarter model was considered. Each element was controlled by an independent design variable. The objective was to minimize the structural weight and the maximum nodal displacement (node 1) subject to normal stress constraints. The limits on the normal stresses were 30000.0 psi. A uniform plate with thickness equal to 0.5 in was taken as the initial design, which resulted in an initial weight of 1.25 lb with a corresponding maximum displacement (node 1) of 0.037 in and a design that was in the feasible region. The lower bound on the design variables was 0.1 in. The MCS algorithm generated five possible solutions. Table 5.7.1 shows the five possible designs and their respective system reliability. The best possible design selected was the one at iteration 29. Figure 5.7.2 plots the MCS algorithm and the constraint method Pareto solutions. One will notice that for this particular problem MCS performed extremely well. The optimal thickness distribution is shown in Table 5.7.2

5.8 Example 8 : Square Plate with Internal and Edge Supports

The final plate problem was a square plate with dimensions 12 in × 12 in (Figure 5.8.1). The plate is supported along its edges and also at internal locations to represent a platform structure with several internal supports (a total of 88 simply supported nodes out of 169 nodes). The plate can be considered to have been made up of nine blocks. The material properties are those of Aluminum with Young's Modulus, $E = 10^7 psi$, Poisson's ratio, $\nu = 0.3$, and mass density, $\rho_m = 2.587 \times 10^{-04} \frac{lbs^2}{in^4}$. The plate was modelled with 144 elements as a complete plate

.

because of the inherent properties of the plate. The first mode shape of the plate has a quarter symmetry. The second and the third modes have diagonal skewed symmetry and the fourth mode has diagonal symmetry. Figure 5.8.3 shows the mode shapes corresponding to the first and second natural frequencies. A total of 24 lb of non-structural mass was added to the structure at all the free nodes. At the initial design all the variables were taken as 1.0 in, which resulted in an initial weight of 38.4 lb with the resulting fundamental frequency $\omega_1 = 29816.384$ $\frac{rad}{sec}$. The plate was optimized for minimum weight and maximum fundamental frequency subject to constraints on the second and third natural frequency. The two constraints were posed as $\omega_2 \geq 35000.0$ $\frac{rad}{sec}$ and $\omega_3 \geq 40000.0$ $\frac{rad}{sec}$. A minimum gauge value of 0.1 in was imposed on all the design variables. The initial design was in the infeasible region. The Pareto optimal solutions for the problem using the MCS algorithm and the Constraint method are plotted in Figure 5.8.2. Table 5.8.1 shows the possible designs with their system reliability. From table 5.8.1 the best design selected is at iteration 38. Constraint two was active at the optimum. At this design an increase of 1.2% in the weight brought about a 5 % increase in the fundamental frequency. Table 5.8.2 gives the first four frequencies at the initial and optimum designs. Table 5.8.3 shows the optimal thickness distribution values for the optimal design. In general, elements at the center of each block were thicker than the others.
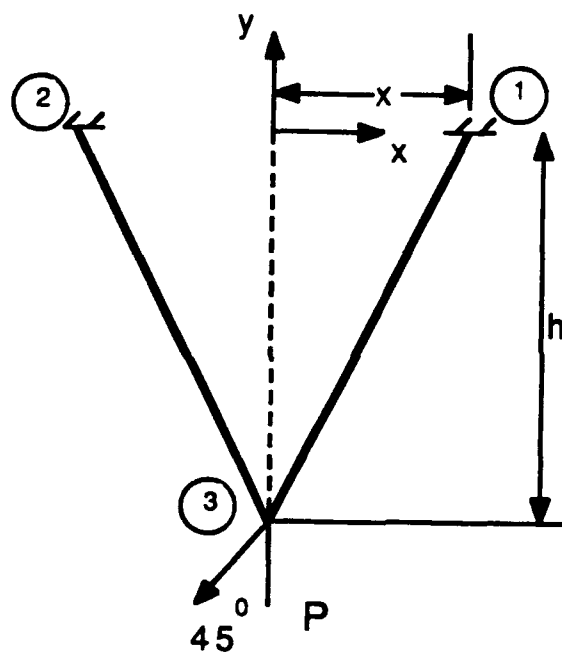
Fig. 5.1.1 Two bar truss structure

Table 5.1.1

Two bar truss - Pareto optimum set

Iter No.	Reliability	Objective Func.
6	0.4996	[68.38, 0.328]
7	1.0000	[86.76, 0.115]
8	1.0000	[81.86, 0.041]

(a)

Quantity	Weighting Method Rao (1987)	Game Theory Rao (1987)	Present Approach
$X=x_1$	0.7635	0.7681	0.8586
x_2	1.0540	1.1408	1.0972
$F=F_1$	75.0595	81.4137	81.8609
F_2	0.0442	0.0408	0.0414
s_1	9747.6	8996.0	9194.0
s_2	1306.9	1180.1	698.0
Reliability	1.0000	1.0000	1.0000

(b)

Space of Design variables

$200 - 1.25 x_1 - 0.75 x_2 \geqslant 0$

$150 - x_2 \geqslant 0$

$200 - x_1 - x_2 \geqslant 0$

(a)

Space of objective functions with Pareto set F^p

F^p

(b)
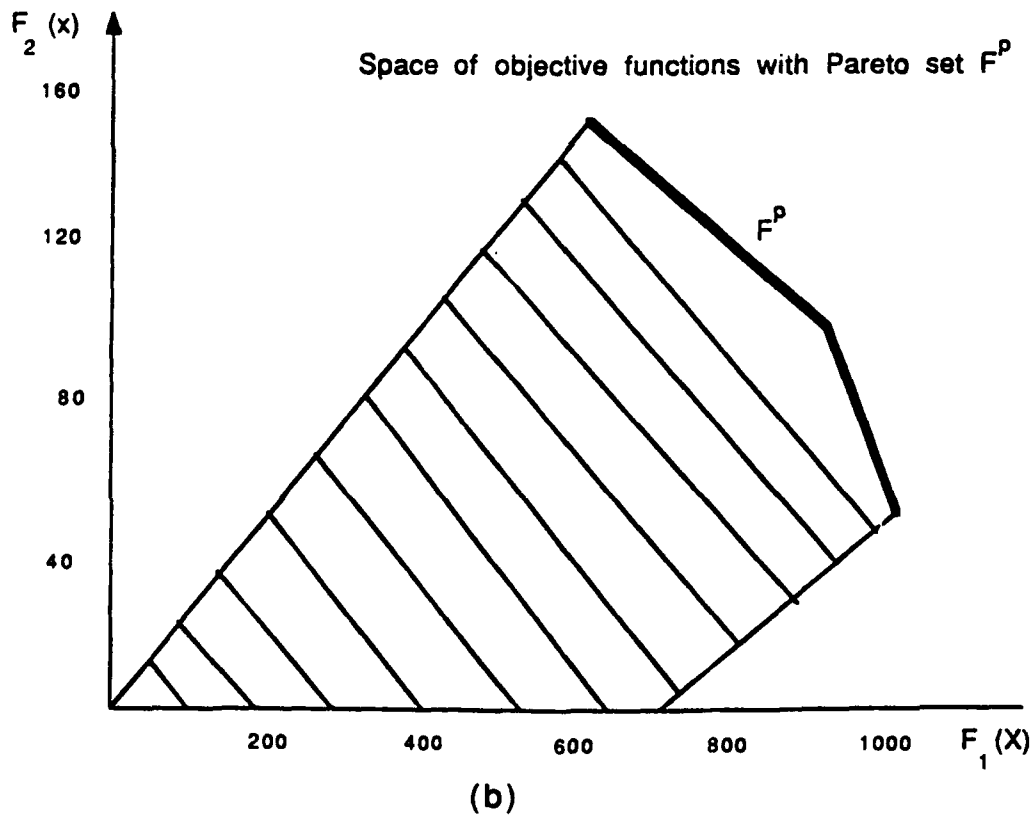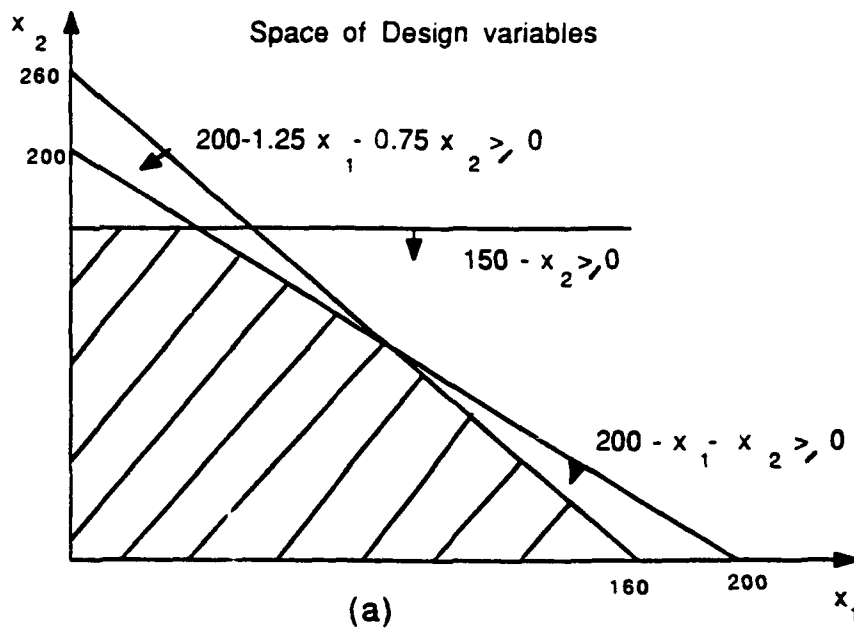
Fig. 5.2.1 Production Planning Problem

Table 5.2.1

Production planning problem - Pareto optimum set

Iter No.	$x = [x_1, x_2]$	$F(x) = [F_1(x), F_2(x)]$	Active Constraint
4	[70.58, 129.41]	[929.41, 70.58]	1
7	[81.07, 118.92]	[918.92, 81.07]	1
9	[92.02, 107.97]	[907.97, 92.02]	1
11	[102.35, 96.08]	[889.81, 102.35]	2
13	[110.30, 82.83]	[855.36, 110.30]	2
15	[117.60, 70.65]	[823.70, 117.60]	2
17	[124.18, 59.68]	[795.18, 124.18]	2
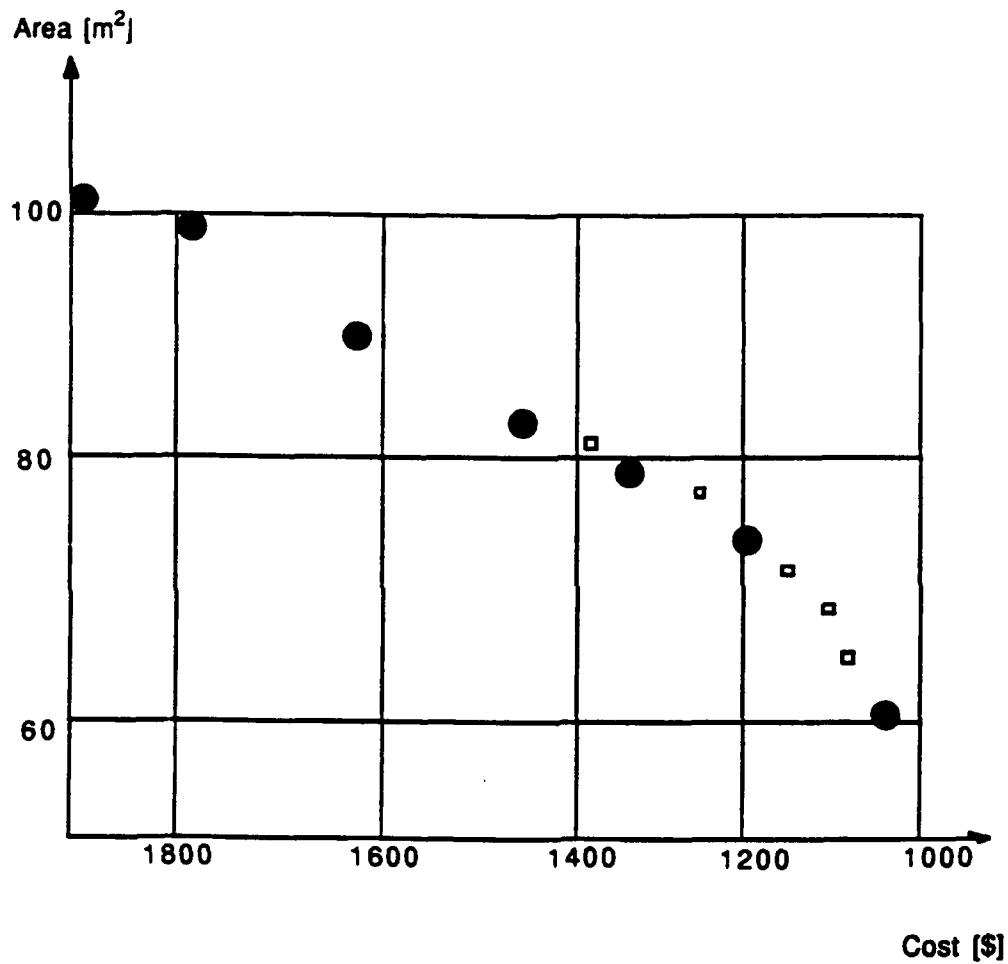
Fig. 5.3.1 Pareto optimal solution for the Apartment problem

Table 5.3.1

Apartment Problem - Pareto optimum set

Pareto-optimal Solutions		
Solution No.	Area [m]^2	Costs [units]
1	79.06	1248.56
2	78.26	1212.12
3	73.89	1169.26
4	71.58	1133.54
5	65.08	1068.39
6	61.09	1028.46

Design Variable [m]					
Solution No.	x_1	x_2	x_3	x_4	x_5
1	3.61	2.65	4.52	2.11	3.70
2	3.51	2.65	4.52	1.74	3.70
3	3.68	1.87	4.52	1.68	3.70
4	3.51	1.84	4.41	1.64	3.70
5	3.51	1.84	3.53	1.64	3.70
6	3.51	1.84	2.99	1.64	3.70

Fig. 5.4.1 Cantilever Beam
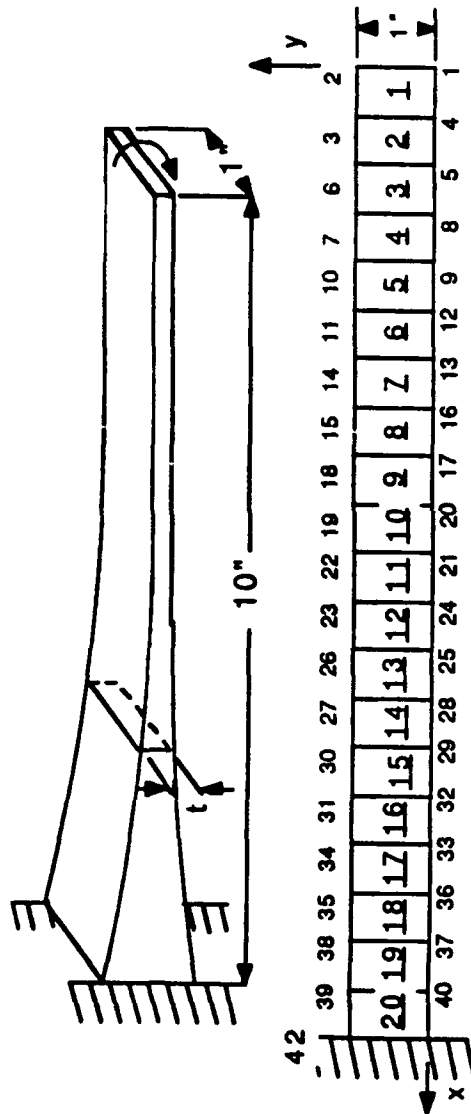
Material Properties
E = 1.0E07
ν = 0.3
ρ = 0.1 lb / in^3

End Moment 450 lb-in

Minimize Weight
Maximize ω_1
Subject to
u $\leq$ 0.5 in
$\sigma \leq$ 30,000.0 psi
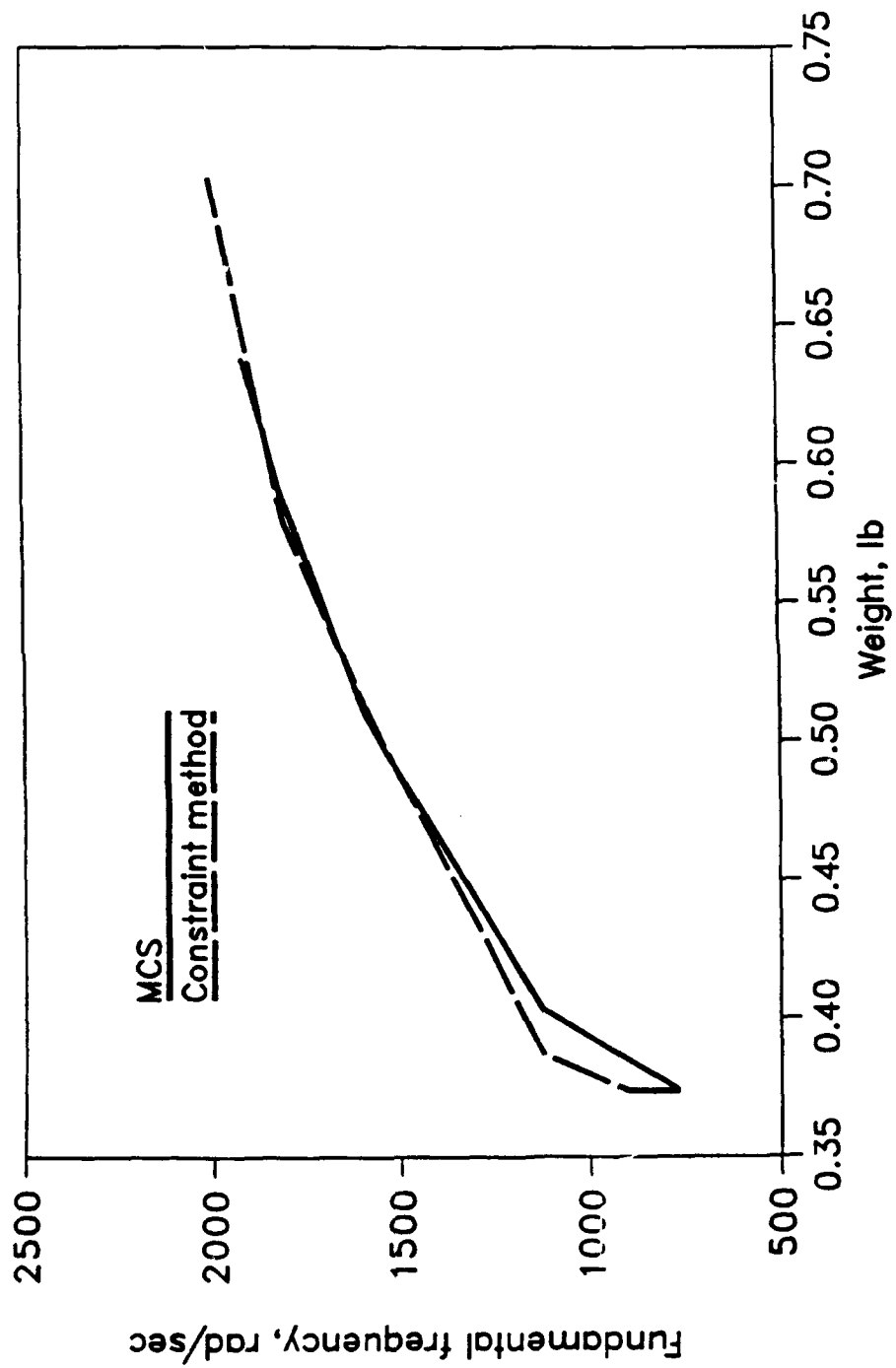
Fig. 5.4.2 Minimal curve in criterion space (Example 4)

y-axis: Fundamental frequency, rad/sec (500, 1000, 1500, 2000, 2500)

x-axis: Weight, lb (0.35, 0.40, 0.45, 0.50, 0.55, 0.60, 0.65, 0.70, 0.75)

Legend:
MCS
Constraint method

Table 5.4.1
Pareto optimal solutions for Cantilever beam

No.	System Reliability	$f(x) = [f(x_1), f(x_2)]$
6	0.0111	[.403, 1123.36]
8	0.0078	[.576, 1885.20]
12	0.0078	[.591, 1956.00]
14	0.0078	[.586, 1984.00]
26	0.0078	[.574, 1973.36]

	Initial	Minimize Wt. Subject to Constraints	Maximize ω_1 Subject to Constraints
Wt. (lb)	0.50	0.37	0.78
ω_1 rad/sec	999.08	770.85	2375.79
System Reliability	0.0000	0.2086	0.0078

Table 5.4.2
Optimal design of Cantilever Beam

Element Number	Iteration No. 6	Iteration No. 8
1	0.3000	0.3000
2	0.3000	0.3000
3	0.3000	0.3000
4	0.3000	0.3000
5	0.3000	0.3000
6	0.3000	0.3000
7	0.3027	0.3000
8	0.3784	0.4873
9	0.3784	0.6092
10	0.4730	0.6092
11	0.4730	0.7614
12	0.4730	0.7614
13	0.4730	0.7614
14	0.4730	0.7614
15	0.4730	0.8184
16	0.4730	0.8184
17	0.4730	0.8184
18	0.4730	0.8184
19	0.4730	0.8184
20	0.4730	0.8184
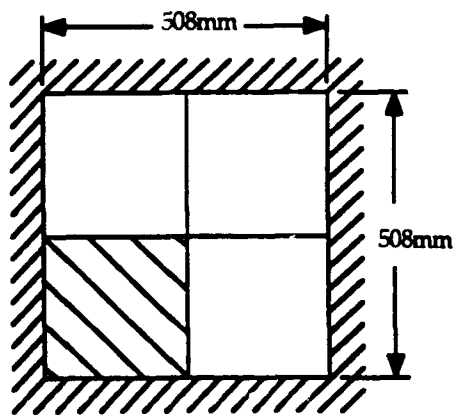
Material Properties:
E = 72.4 GPa
$\upsilon = 0.3$
$\rho = 2.77\,gm/cm^3$

UDL=110.3kPa

(a)
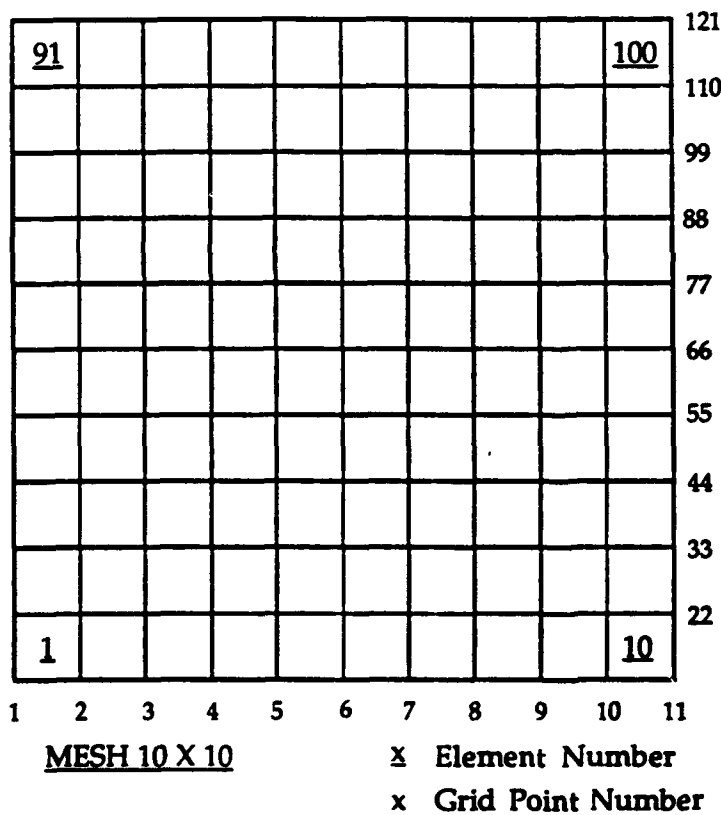
Optimization Problem:

Minimize Weight
Min. u(121)
Subject to
$\sigma < 82.7\,MPa$

MESH 10 X 10

$\underline{X}$ Element Number

x Grid Point Number

(b)

Fig. 5.5.1 Clamped Square Plate With Uniform
Lateral Load
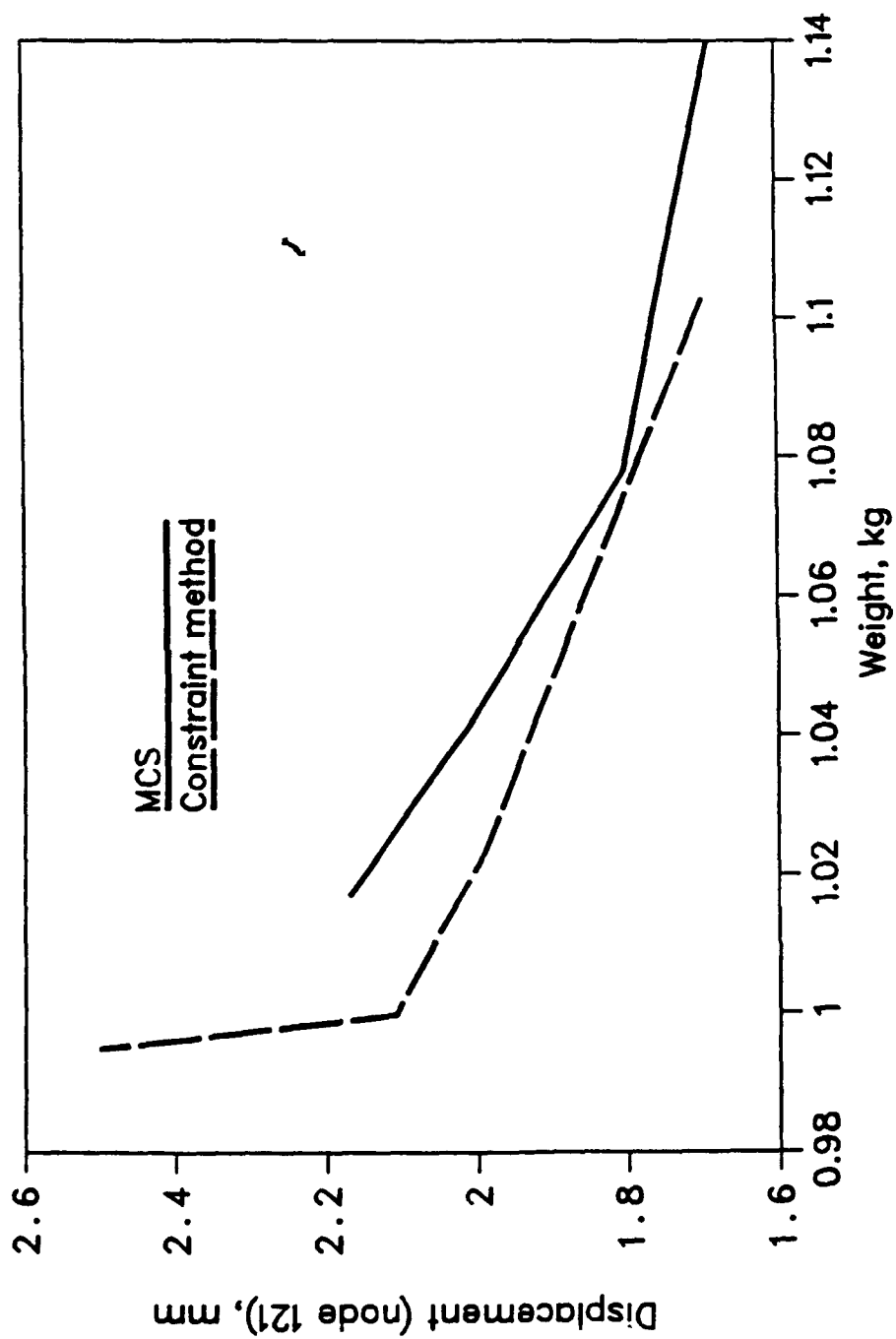
Fig. 5.5.2 Minimal curve in criterion space (Example 5)
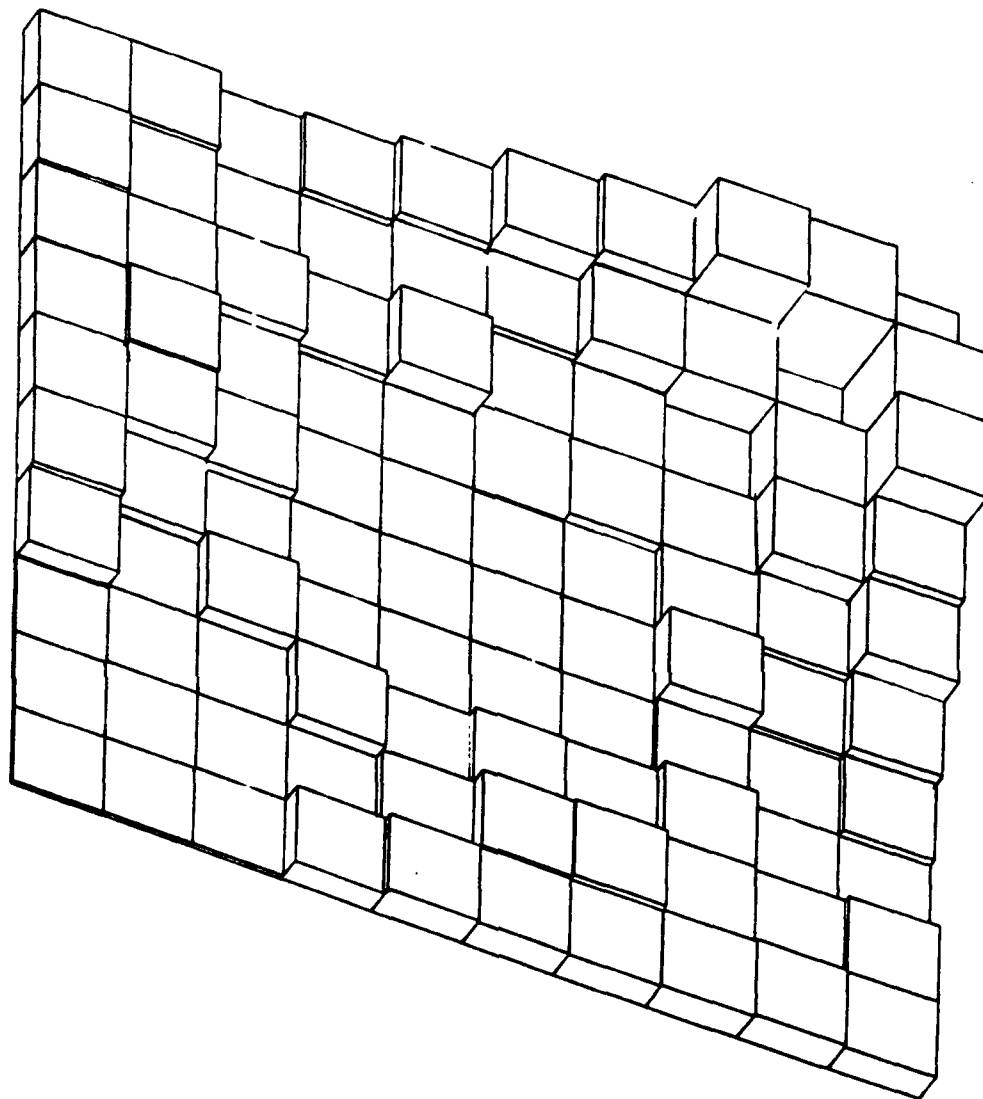
Fig. 5.5.3 Optimal Design (Example 5)

Table 5.5.1
Pareto optimal solutions for the Clamped Square Plate

Iter No.	System Reliability	$f(x) = [f_1(x), f_2(x)]$ [Weight , Displacement]
11	1.0000	[1.2820, 1.7676]
19	0.9905	[1.2426, 1.9190]
28	0.8518	[1.1820, 1.9792]
29	0.9918	[1.1838, 1.9717]

	Initial	Minimize Wt. Subject to Stress constraints	Minimize maximum displacement Subject to Stress constraints
Wt. (Kg)	1.36	0.99	11.06
u (mm)	3.1517	2.49	0.69
System Reliability	0.0000	0.7628	1.0000

Table 5.5.2
Optimal design of Clamped square plate

Ele No.	Thickness	Ele. No.	Thickness
1	1.2517	51	8.9890
2	1.2517	52	9.8852
3	1.2517	53	4.6286
4	7.5306	54	1.5204
5	9.4372	55	1.4176
6	8.9890	56	1.0000
7	8.7843	57	1.4664
8	9.1833	58	5.1504
9	9.9334	59	7.3205
10	9.1833	60	17.4012
11	1.2517	61	8.7843
12	1.2517	62	10.6869
13	1.7093	63	4.4490
14	1.5636	64	1.4664
15	4.7489	65	1.4664
16	9.8852	66	1.4664
17	10.6869	67	4.4643
18	8.6516	68	4.7489
19	7.6358	69	14.9552
20	9.3592	70	20.4048
21	1.2517	71	9.1833
22	1.7093	72	8.6516
23	1.4676	73	8.4229
24	6.4603	74	3.5196
25	1.5636	75	10.2041
26	4.6286	76	5.1504
27	4.4490	77	4.7489
28	8.4229	78	1.0000
29	3.3411	79	14.9552
30	3.3411	80	32.0786
31	7.5306	81	9.9334
32	1.5636	82	7.6358
33	6.4603	83	3.3411
34	1.7722	84	3.3411
35	1.4664	85	5.1504
36	1.5204	86	7.3205
37	1.4664	87	14.9552
38	3.5196	88	14.9552
39	3.3411	89	1.0000
40	5.6592	90	29.4741
41	9.4372	91	9.1833
42	4.7489	92	9.3592
43	1.5636	93	3.3411
44	1.4664	94	5.6592
45	1.4697	95	9.2838
46	1.4176	96	17.4012
47	1.4664	97	20.4048
48	10.2041	98	32.0786
49	5.1504	99	29.4741
50	9.2838	100	13.9009
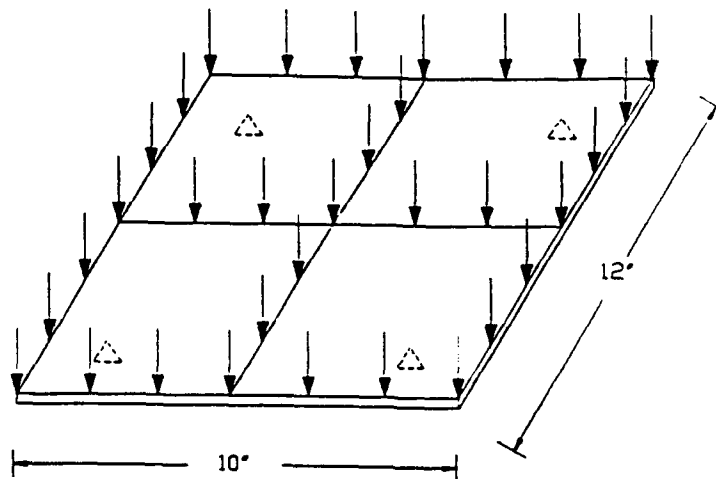
Material Properties

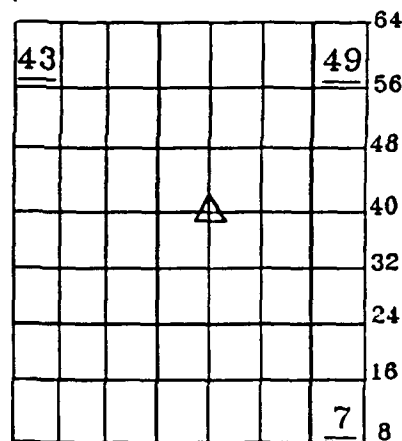$E = 28.E07$ psi

$\nu = 0.3$

$\rho_s = 7.71E\text{-}04$ lb s²/ in⁴

Minimize Weight
Maximize ω_1

Subject to
$u < 0.02$ in
$\sigma < 25000.0$ psi

Quarter Model

Fig. 5.6.1 Plate Supported Along Four Diagonal Points
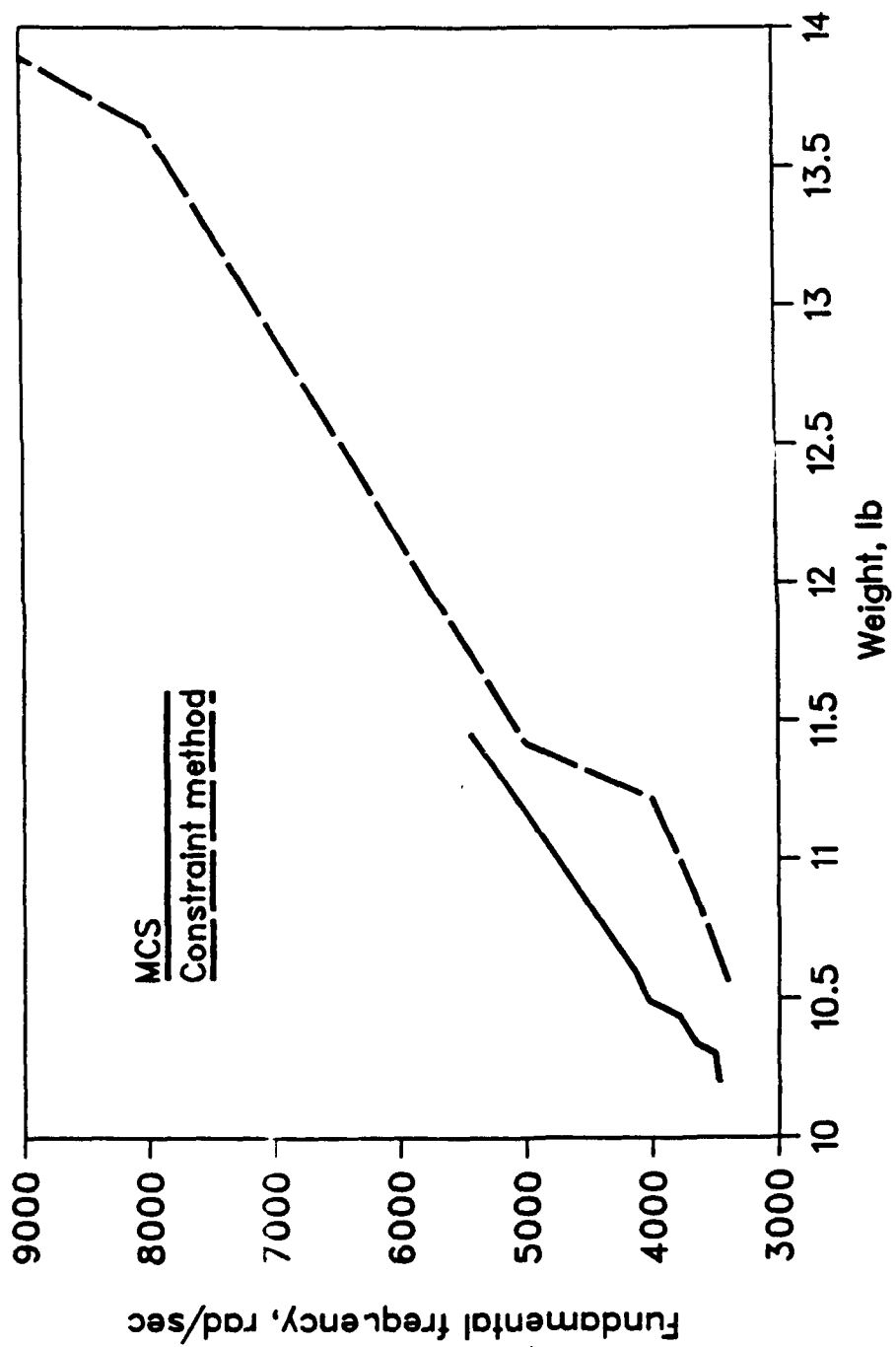
Fig. 5.6.2 Minimal curve in criterion space (Example 6)
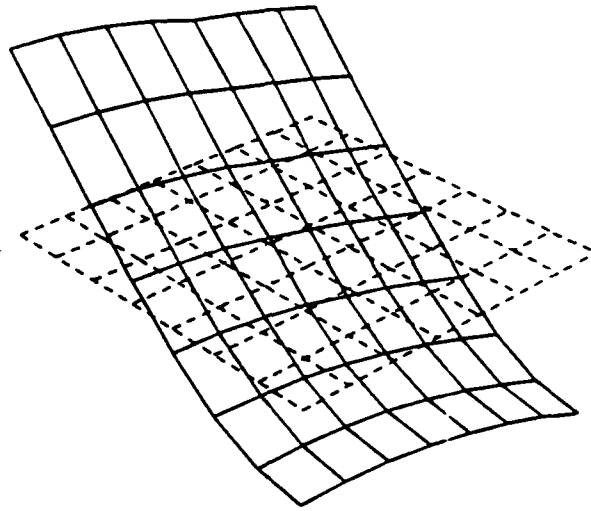
(a) Mode 1
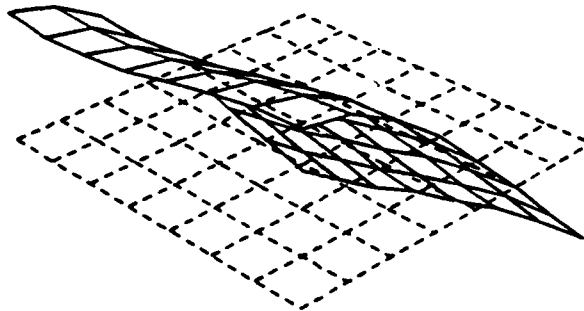
(b) Mode 2

Fig. 5.6.3 Mode shapes for Example 6
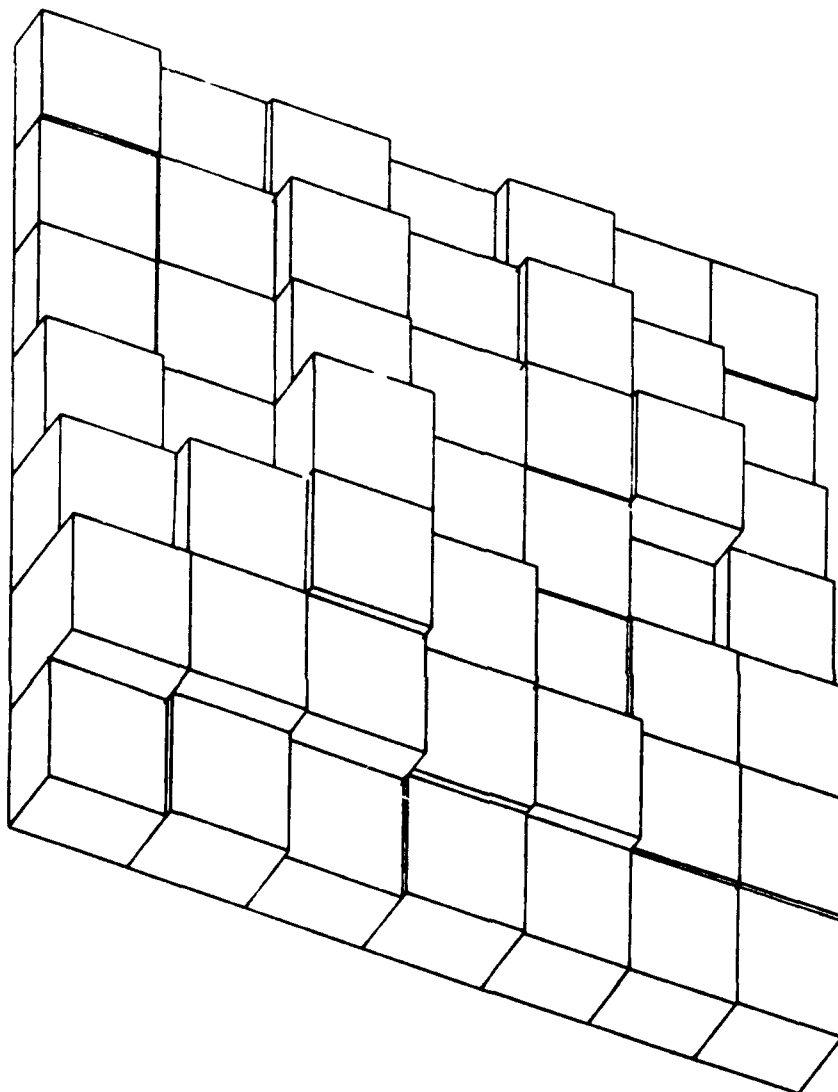
Fig. 5.6.4 Optimal Design (Example 6)

Table 5.6.1
Load condition data for Example 6

Node Number(s)	Load condition	Applied nodal forces, in Pounds
1		357.34
2-7		142.86
8		200
9,17,25,33,41,49		171.43
57,64		192.86
58-63		214.86
16,24,32,40,48,56		257.14

Table 5.6.2

Pareto optimal solutions for the Plate with
Four Diagonal supports

Iter No.	System Reliability	$f(x) = [f(x_1), f(x_2)]$
19	0.5357	[10.34, 3651.89]
22	0.5337	[10.44, 3793.82]
25	0.5459	[10.50, 3897.54]
28	0.5394	[10.62, 4061.11]
31	0.9116	[10.26, 3725.74]
34	0.4959	[10.29, 3788.21]
36	0.4631	[10.40, 3923.56]
38	0.4615	[10.49, 4033.87]

	Initial	Minimize Wt. Subject to Constraints	Maximize ω_1 Subject to Constraints
Wt. (lb)	12.35	9.26	14.56
ω_1 (rad/sec)	5400.34	1924.00	8758.00
System Reliability	1.0000	0.3423	1.0000

Table 5.6.3
First Five Frequencies (Example 6)

	Initial	Optimal
ω_1	5400.338	3672.200
ω_2	8157.842	4420.065
ω_3	13307.113	6790.055
ω_4	17350.319	8775.119
ω_5	19396.273	11241.834

Table 5.6.4
Optimal design of Plate with four diagonal supports

Ele No.	Thickness	Ele. No.	Thickness
1	0.5014	25	0.5034
2	0.5515	26	0.4932
3	0.5014	27	0.2222
4	0.5459	28	0.3949
5	0.5292	29	0.3151
6	0.5249	30	0.3268
7	0.5362	31	0.5456
8	0.7735	32	0.4857
9	0.7710	33	0.5081
10	0.7621	34	0.5612
11	0.6089	35	0.2866
12	0.6503	36	0.3151
13	0.5578	37	0.3279
14	0.5581	38	0.5106
15	0.5969	39	0.4027
16	0.7483	40	0.5081
17	0.8349	41	0.3083
18	0.6627	42	0.1296
19	0.4836	43	0.3397
20	0.5186	44	0.2075
21	0.5106	45	0.2561
22	0.4107	46	0.1050
23	0.3268	47	0.2566
24	0.8349	48	0.1481
		49	0.1467

(a)
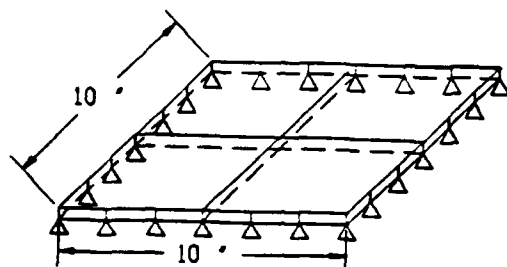
Material Properties:

E = 1.0E07 psi
υ = 0.3
ρ = 0.1 lb/in^3
Udl = 100 psi
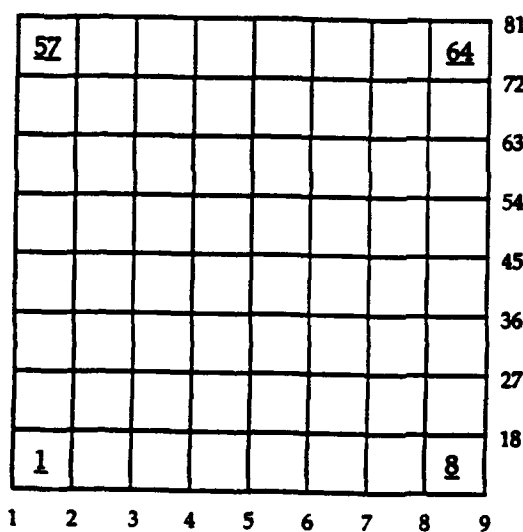
Optimization:

Minimize Wt.
Minimize u(1)

Subject to
$\sigma \leqslant 30000.0$ psi

MESH 8 X 8 $\underline{x}$ Element Number

x   Grid Point Number

(b)

Fig. 5.7.1   Simply Supported Square Plate

102
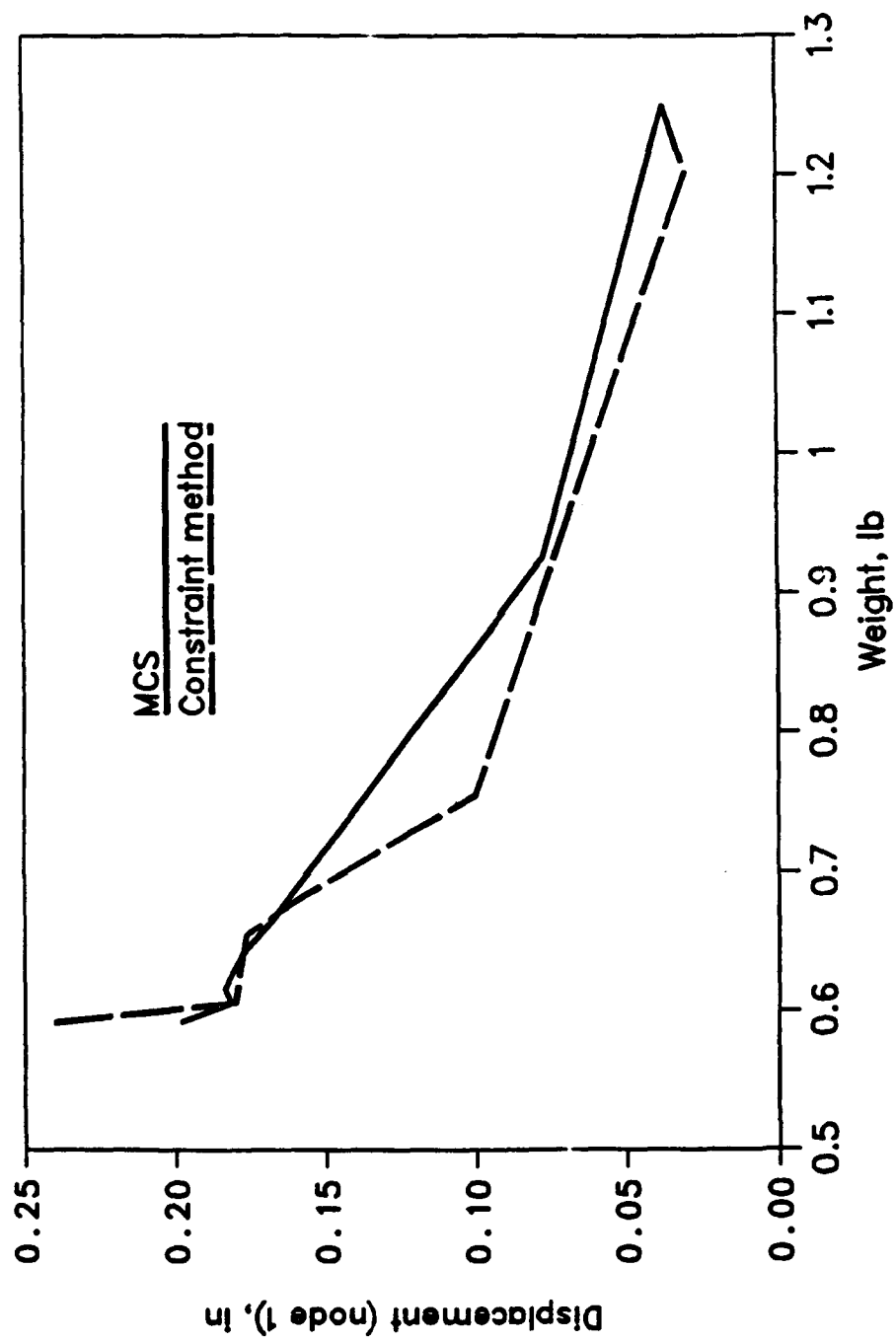
Fig. 5.7.2 Minimal curve in criterion space (Example 7)

Table 5.7.1
Pareto optimal solutions for square plate
simply supported at the edges

Iter No.	System Reliability	$F(x) = [\, F_1(x), F_2(x)\,]$ [Weight , Displacement]
11	0.0247	[0.7119, 0.1608]
17	0.0101	[0.6852, 0.1674]
23	0.0196	[0.6630, 0.1727]
29	0.0895	[0.6401, 0.1779]
36	0.0211	[0.6167, 0.1836]

	Initial	Minimize Wt. Subject to Stress constraints	Minimize Maximum Displacement Subject to Stress constraints
Wt. (lb)	1.2500	0.5915	1.2500
u (in)	0.0372	0.2423	0.0372
System Reliability	1.0000	0.0010	1.0000

Table 5.7.2
Optimal design of simply supported square plate

Ele No.	Thickness	Ele. No.	Thickness
1	0.2870	33	0.2709
2	0.3108	34	0.2353
3	0.3182	35	0.1829
4	0.3121	36	0.2176
5	0.2709	37	0.1260
6	0.1933	38	0.1554
7	0.1505	39	0.4918
8	0.1260	40	0.3061
9	0.3108	41	0.1933
10	0.2603	42	0.2173
11	0.3121	43	0.2139
12	0.2870	44	0.1933
13	0.2353	45	0.1554
14	0.2173	46	0.3958
15	0.1751	47	0.4918
16	0.1505	48	0.3627
17	0.3182	49	0.1505
18	0.3121	50	0.1751
19	0.2710	51	0.2419
20	0.3121	52	0.2531
21	0.1829	53	0.4918
22	0.2139	54	0.4918
23	0.2419	55	0.4918
24	0.1751	56	0.2531
25	0.3121	57	0.1260
26	0.2870	58	0.1505
27	0.3121	59	0.1751
28	0.1484	60	0.2273
29	0.2176	61	0.3061
30	0.1933	62	0.3627
31	0.2531	63	0.2531
32	0.2273	64	0.1333

Material Properties:

E = 1.0E07 psi

ν = 0.3
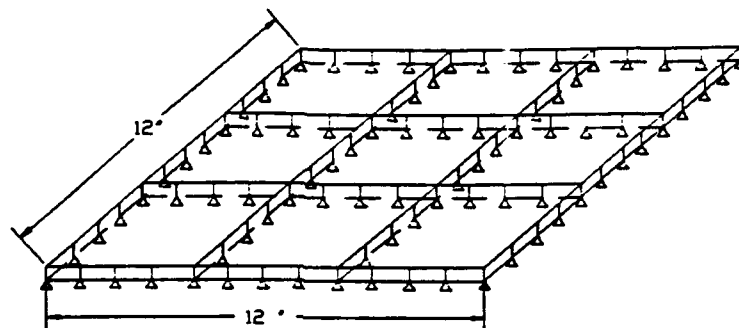
ρ_m = 2.587E-04 lb s^2/ in^4

Minimize Wt

Maximize ω_1

Subject to
$\omega_2 \geq$ 35000.0 rad/sec
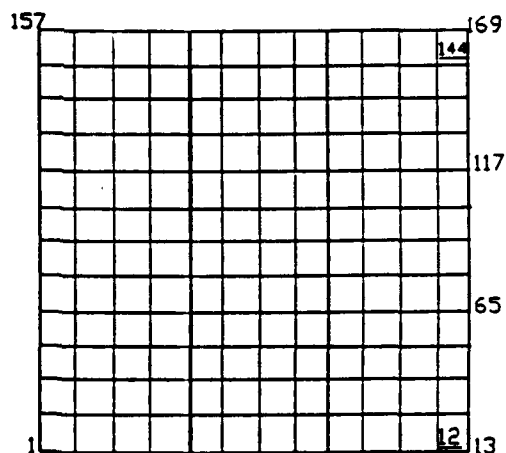
$\omega_3 \geq$ 40000.0 rad/sec

Fig 5.8.1. SQUARE PLATE WITH INTERNAL
AND EDGE SUPPORTS
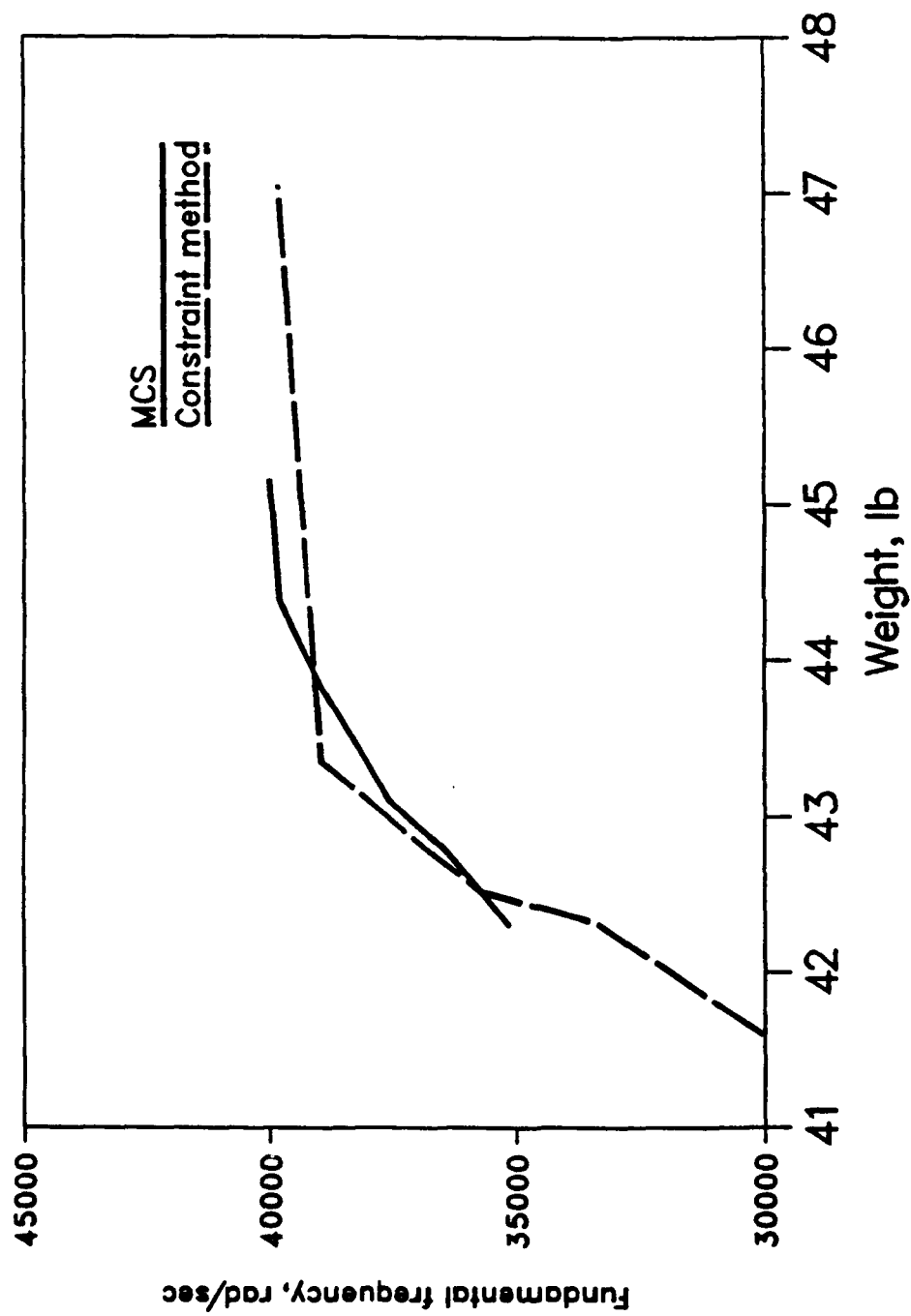
Fig. 5.8.2 Minimal curve in criterion space (Example 8)
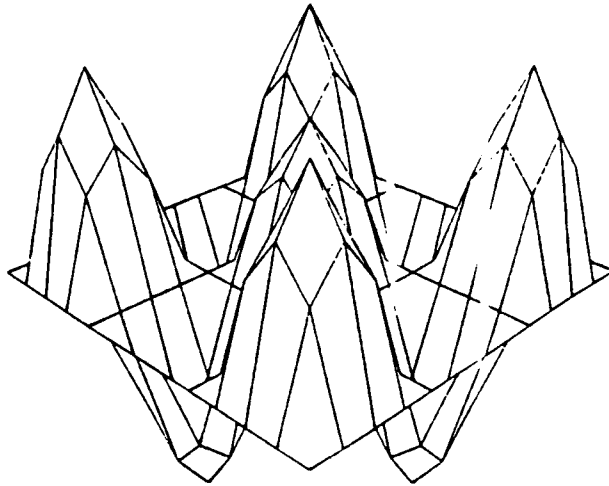
Mode 1
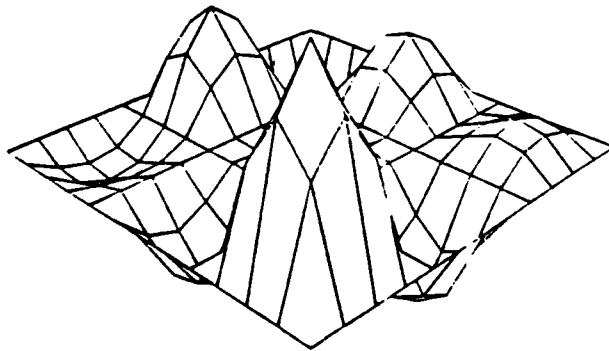
Mode 2

Fig. 5.8.3 Mode shapes for Example 8

Table 5.8.1

Pareto optimal solutions for square plate with internal and edge supports

Iter No.	System Reliability	$F(x) = [F_1(x), F_2(x)]$ [Weight, Fundamental Frequency]
38	0.9379	[42.88, 36461.20]
29	0.9?11	[43.65, 36859.02]
28	0.9·10	[43.77, 37549.32]
24	0.9299	[43.82, 38906.14]
34	0.0212	[44.36, 39777.20]

	Initial	Minimize Weight Subject to Constraints on ω_2, ω_3	Maximize ω_1 Subject to Constraints on ω_2, ω_3
Wt. lb	38.4	42.?2	63.82
ω_1 (rad/sec)	29816.38	33404.12	43610.63
System Reliability	0.0000	0.0235	1.0000

Table 5.8.2

First Four natural frequencies

	Minimze Wt. Subject to constraints on ω_2, ω_3	Maximize ω_1 Subject to constraints on ω_2, ω_3	Optimum Design
ω_1	33404.116	43610.631	36461.208
ω_2	36647.414	45184.092	37479.610
ω_3	39899.018	48042.382	40026.954
ω_4	39975.613	52362.123	40539.290

110

Table 5.8.3
Optimal design of Plate with internal and edge supports

Ele. No.	Thickness	Ele No.	Thickness	Ele No.	Thickness
1	1.5455	49	2.1182	97	2.0005
2	1.3769	50	1.7226	98	1.5276
3	0.9866	51	1.9478	99	0.6417
4	1.5432	52	1.7475	100	0.8290
5	1.3185	53	1.1854	101	2.5997
6	0.5840	54	1.5957	102	0.8326
7	0.5829	55	1.2392	103	0.8961
8	1.2392	56	0.7162	104	1.5637
9	0.6029	57	1.5035	105	0.7680
10	1.5407	58	0.9267	106	0.9892
11	1.5407	59	1.7039	107	1.0407
12	0.6958	60	1.2638	108	1.7713
13	1.4602	61	0.6406	109	0.7697
14	1.4881	62	1.7226	110	1.6664
15	0.9866	63	1.9478	111	1.4670
16	1.5349	64	1.0395	112	1.5184
17	1.5356	65	1.3897	113	0.9401
18	1.5435	66	0.9089	114	1.2647
19	1.4321	67	0.8087	115	0.8938
20	1.5532	68	1.4660	116	1.1506
21	1.5727	69	0.8833	117	0.4936
22	1.5380	70	1.0306	118	1.0234
23	1.3450	71	1.9909	119	1.1669
24	1.3450	72	1.1324	120	1.2182
25	1.6935	73.	0.6406	121	1.5895
26	1.8253	74	1.5135	122	1.7711
27	1.5105	75	0.8909	123	1.6871
28	0.8078	76	0.9013	124	1.3356
29	0.7034	77	1.4269	125	1.6359
30	0.6529	78	0.9847	126	1.6167
31	1.3526	79	0.9847	127	1.7606
32	1.5543	80	1.5178	128	1.6365
33	1.5497	81	0.7769	129	1.6328
34	1.6788	82	1.3558	130	1.4934
35	1.4394	83	1.5315	131	1.2482
36	0.6036	84	1.1109	132	1.0246
37	2.2266	85	2.1140	133	1.7956
38	1.6850	86	1.5389	134	1.6306
39	1.9858	87	0.9954	135	1.6306
40	1.6083	88	1.8455	136	0.7917
41	2.2096	89	1.1092	137	1.1763
42	0.9300	90	1.2965	138	0.7624
43	0.6553	91	1.2857	139	0.7123
44	2.1413	92	0.7885	140	1.1629
45	0.5522	93	1.5548	141	1.4388
46	0.5609	94	1.0442	142	1.2911
47	1.2521	95	1.1451	143	1.2100
48	1.3595	96	1.1151	144	1.7864

111

SECTION 6

CONCLUSIONS

A new technique for multiobjective optimization was developed. An effort was made to modify the existing Generalized compound scaling algorithm for multiobjective optimization techniques. This technique was demonstrated on large scale problems with more than one hundred design variables and above three hundred constraints. Objective functions which were linear as well as non-linear were used for demonstration of the multiobjective algorithm. Complete Pareto solution sets were generated for the problems using the constraint method for comparison with the present approach. In most of the problems the MCS Pareto set followed quite closely to the constraint method. The technique proved to be robust as well as computationally efficient. The best compromise design was selected based on the system reliability of the structure. This proved to be an efficient way for selecting the best possible compromise solution. As in most structural optimization problems the optimum lies on the constraint boundary of the active constraint or at the intersection of the active constraints. This assumption was the basis in developing the algorithm. Pareto optimal solutions also lie on the constraint surface, and since the objectives are also treated as constraints, generating Pareto solutions was straight forward.

112

Some of the drawbacks of this method are that Pareto solutions are found only when the solutions lie on the constraint boundary. If this is not the case, then arbitrary solutions are generated which may or may not be Pareto optimal. For some of the problems where one of the objective functions is highly non-linear (frequency), the MCS generated solutions crossed over the constraint method curves hence generating solutions which were not true Pareto optimum. This was seen for Example 8 where the number of design variables was 144. This was not seen for cases when weight and displacements were used as the conflicting objective functions. On the whole when comparing MCS to the methods described in Section 1 (eg., constraint, weighting, NISE, global criterion methods), the algorithm proved to be reliable and robust requiring less computer resources to generate a Pareto set. Validation of this technique on plate structures with displacement, stress, and frequency functions (constraints or objectives) where the problems are highly nonlinear demonstrated the algorithms capabilities.

REFERENCES

Balachandran, M., and Gero, J.S., 1987: Use of knowledge in selection and control of optimization algorithm. *Enginee ing Optimization, Vol. 12, No. 2, 163-173.*

Bartel, D.L., and Marks, R.W., 1974: The optimum design of mechanical systems with competing design objectives. *Journal of Engineering for Industry, Vol. 96, 171-178.*

Belytschko, T., Tsay, C.S., and Liu, W.K., 1981: A stabilization matrix for the bilinear Mindlin plate element. *Computational Methods in Applied Mechanics and Engineering, Vol. 29, No.3, 313-327.*

Belytschko, T., and Tsay, C.S., 1983: A stabilization procedure for the quadrilateral plate element with one-point quadrature. *International Journal for Numerical Methods in Engineering, Vol.19, No.3, 405-419.*

Brockman, R.A., 1987: Dynamics of the bilinear Mindlin plate element. *International Journal for Numerical Methods in Engineering, Vol.24, No.12, 2343-2356.*

Brockman, R.A., Lung, F.Y., and Braisted W.R., 1989: Probabilistic finite element analysis of dynamic structural response. *WPAFB, Technical Report,*

AFWAL-TR-88-2149.

Cohon, J.L., 1978: Multiobjective programming and planning. *Academic Press, New York.*

Cook, R.D., Malkus, D.S., and Plesha, M.E., 1989: Concepts and applications of finite element analysis (Third Edition). *John Wiley and Sons, 190-192.*

Davidson, J.W, Felton, L.P, and Hart, G.C., 1977: Optimum design of structures with random parameters. *Computers and Structures, Vol. 7, 481-486.*

Diaz, A., 1987: Interactive solution to multiobjective optimization problem. *International Journal for Numerical Methods in Engineering, Vol. 24, 1865-1877.*

Dhingra, A.K., Rao, S.S., and Miura, H., 1990: Multiobjective decision making in a fuzzy environment with applications to helicopter design. *AIAA Journal, Vol. 28, 703-710.*

Duckstein, L., 1984: Multiobjective optimization in structural design: The model choice problem. *In E. Atrek et.al. (eds.), New Directions in Structural Design, Wiley, New York.*

El-Sayed, M.E.M, Ridgely, B.J., and Sandgren, E., 1989: Nonlinear structural optimization using goal prograring. *Computers and Structures, Vol. 32, No.1, 69-73.*

Eschenauer, H., Koski, J. and Osyczka, A., 1990: Multicriteria design optimization, Procedures and Applications. *Springer, Verlag, Berlin, Hedelberg.*

Grandhi, R.V., Venugopal, N.S., and Venkayya, V.B., 1991: Optimality criteria method for minimum weight design of plate structures. *32nd AIAA /ASME /ASCE /AHS /ASC Structures, Structural Dynamics, and Material Conference, Baltimore, MD, Part 1, AIAA-91-0923, 213-226.*

Hajela, P. and Shih, C.J., 1990: Multiobjective optimum design in mixed integer and discrete design variable problem. *AIAA Journal, Vol. 28, 670-675.*

Hughes, T.J.R, Cohen, M. and Haroun, M., 1978: Reduced and selective integration techniques in finite element analysis of plates. *Nuclear Engineering Design, Vol. 46, 203-222.*

Hwang, C.L. and Masud, A.S.M., 1979: Multiple objective decision making - Methods and Applications. *Springer, Verlag, Berlin.*

Koski, J. and Silvennoinen, R., 1982: Pareto optima of isostatic trusses. *Computational Methods in Applied Mechanical Engineering, Vol. 31, No. 3, 265-279.*

Koski, J., 1984: Bicriterion optimum design method for elastic trusses. *Acta Polytechnica Scandinavica, Mechanical Engineering Series No. 86, Helsinki.*

Koski, J., 1987: Norm methods and partial weighting in multicriterion optimization of structures. *International Journal for Numerical Methods in Engineering,*

116

Vol. 24, No. 21, 1101-1121.

Koski, J., 1981: Multicriteria optimization in structural design. *International Symposium on Optimum Structural Design: The 11th ONR Naval Structural Mechanics Symposium, Tucson, Arizona.*

Koski, J., 1984: Multicriterion optimization in structural design. *In E. Atrek et.al. (eds.), New Directions in Structural Design, Wiley, New York, 483-503*

Kuhn, H.W. and Tucker A.W., 1951: Nonlinear programming. *In Proceedings of the Second Berkeley Symposium on Mathematical Statistics and Probability. (Edited by J. Neyman), 481-491.*

Mindlin, R.D., 1951: Influence of rotary inertia and shear on the bending of elastic plates. *Journal of Applied Mechanics, Vol. 18, 1031-1036.*

Nikolaidis, E., and Burdisso, R., 1988: Reliability based optimization: A safety index approach. *Computers and Structures, Vol. 28, No. 6, 781-788.*

Osyczka, A., 1984: Multicriterion optimization on engineering. *Ellis Horwood Series in Engineering Sciences.*

Prasad, B., and Haftka, R.T., 1979: Optimum structural design with plate bending finite elements. *ASCE J. Structures Division, Vol. 105, ST11, 2367-2382.*

117

Radford, A.D., Gero, J.S., Rosenman, M.A., and Balachandran, M., 1985: Pareto Optimization as a Computer-Aided lesign tool. *Gero, J.S. (ed): Optimization in Computer-Aided Design. Amsterdam: North-Holland, 47-69.*

Rao, S.S., 1984: Multiobjective optimization in structural design with uncertain parameters and stochastic processes. *AIAA Journal, Vol. 22, No.1, 1670-1678.*

Rao, S.S., 1984: Optimization, Theory and Applications (Second Edition). *John Wiley and Sons, 610-612.*

Rao. S.S., 1987: Game theory approach for multiobjective structural optimization. *Computers and Structures, Vol. 25, 119-127.*

Rao, S.S., Venkayya, V.B., and Khot, N.S., 1988: Optimization of actively controlled structures using goal programming techniques. *International Journal for Numerical Methods in Engineering, Vol 26, No. 1, 183-197.*

Rao, S.S., Venkayya, V.B., and Khot, N.S., 1988: Game Theory approach for the integrated design of structures and controls. *AIAA Journal, Vol. 26, No. 4, 463-469.*

Rao, S.S., Design of vibration isolation systems using multiobjective optimization techniques. *ASME paper, No. 84-DET-60.*

Sandgren, E., 1989: Structural design optimization for latitude by nonlinear goal programming. *Computers and Structures, Vol. 33, No. 6, 1395-1402.*

Saravanos, D.A., and Chamis, C.C., 1990: Multiobjective shape and material optimization of composite structures including damping. *Presented at 31st Structures, Structural Dynamics, and Materials Conference, Long Beach, CA, 2-4 Apr, 371-377.*

Schmit, L.A., and Farshi, B., 1974: Some approximation concepts for structural synthesis. *AIAA Journal, Vol. 12, No. 5, 692-699.*

Stadler, W., 1984: Multicriteria Optimization in Mechanics (A Survey). *Applied Mechanics Reviews, Vol. 37, No. 3, 277-286.*

Stadler, W., 1987: Update to multicriteria Optimization in Mechanics (A Survey). *Applied Mechanics Update, ASME, 417-420.*

Starnes, J.H, and Haftka, R.T., 1979: Preliminary design of composite wings for buckling, stress and displacement constraints. *Journal of Aircraft, Vol. 16, 564-570.*

Tseng, C.H., and Lu, T.W., 1990: Minimax multiobjective optimization in structural design. *International Journal for Numerical Methods in Engineering, Vol. 30, No. 6, 1213-1228.*

Venkayya, V.B., 1971: Design of optimum structures. *Computers and Structures, Vol. 1, 265-309.*

Venkayya, V.B., 1986: A further Generalization of Optimality Criteria Approaches in Structural Optimization. *Proceedings of the International Conference on Computational Engineering Science, April 10-14, Atlanta, Ga., 46i.1-15.*

Venkayya, V.B., and Tischler, V.A., 1989: A compound scaling algorithm for mathematical optimization. *WPAFB Technical Report, WDRC-TR-89-3040.*

Venkayya, V.B., 1989: Optimality Criteria: A basis for multidisciplinary design optimization. *Journal of Computational Mechanics, Vol. 5, 1-21.*

Venkayya, V.B., Kolonay, R.M, Tischler, V.A, and Canfield, R.A., 1990: A generalized optimality criteria for mathematical optimization. *A paper presented at AIAA Dynamics Specialist Conference, Long Beach, CA, April.*

Venkayya, V.B., 1991: Design optimization in dynamic environment. *International Conference on Recent Advances in Structural Dynamics, Southhampton, England, July.*

Whitney, J.M., 1973: Shear correction factors for orthotropic laminates under static load. *Journal of Applied Mechanics, Vol. 40, 302- 304.*

Yang, J.S., and Nikolaidis, E., 1990: Design of aircraft wings subjected to gust loads: A safety index based approach. *AIAA, Vol 29, No.5, 804-812.*

120